



National Assessment of Hurricane-Induced Coastal Erosion Hazards: Northeast Atlantic Coast

By Justin J. Birchler, Hilary F. Stockdon, Kara S. Doran, and David M. Thompson

Open-File Report 2014–1243

U.S. Department of the Interior
U.S. Geological Survey

U.S. Department of the Interior
SALLY JEWELL, Secretary

U.S. Geological Survey
Suzette M. Kimball, Acting Director

U.S. Geological Survey, Reston, Virginia: 2014

For more information on the USGS—the Federal source for science about the Earth, its natural and living resources, natural hazards, and the environment—visit <http://www.usgs.gov> or call 1-888-ASK-USGS

For an overview of USGS information products, including maps, imagery, and publications, visit <http://www.usgs.gov/pubprod>

To order this and other USGS information products, visit <http://store.usgs.gov>

Any use of trade, product, or firm names is for descriptive purposes only and does not imply endorsement by the U.S. Government.

Although this report is in the public domain, permission must be secured from the individual copyright owners to reproduce any copyrighted material contained within this report.

Suggested citation:

Birchler, J.J., Stockdon, H.F., Doran, K.S., and Thompson, D.M., 2014, National assessment of hurricane-induced coastal erosion hazards—Northeast Atlantic Coast: U.S. Geological Survey Open-File Report 2014–1243, 34 p., <http://dx.doi.org/10.3133/ofr20141243>.

ISSN 2331-1258 (online)

Contents

- 1. Introduction..... 1
 - 1.1 Impacts of Hurricanes on Coastal Communities 1
 - 1.2 Prediction of Hurricane-Induced Coastal Erosion..... 4
 - 1.3 Storm-Impact Scaling Model 4
- 2. Methods..... 7
 - 2.1 Lidar-Derived Beach Morphology..... 7
 - 2.2 Hurricane-Induced Water Levels..... 9
 - 2.2.1 Tide and Storm Surge 10
 - 2.2.2 Wave Height and Period..... 12
 - 2.2.3 Wave Setup and Swash 16
 - 2.3 Probability of Coastal Change..... 17
- 3. Results..... 18
 - 3.1 Coastal Morphology 18
 - 3.2 Hurricane-Induced Water Levels..... 25
 - 3.3 Probability of Coastal Change..... 25
- 4. Discussion 28
 - 4.1 Validity of Assumptions 28
 - 4.2 Relative Importance of Waves and Storm Surge 28
 - 4.3 Nor'easters versus Hurricanes 28
 - 4.4 Coastal Morphology 29
 - 4.5 Assessment Updates 29
- 5. Conclusion..... 30
- 6. Acknowledgments..... 30
- 7. References Cited..... 31
- Tables..... 33

Figures

- Figure 1.** Collapsed road in Westport, Massachusetts, as a result of erosion during Hurricane Irene (August 2011) 1
- Figure 2.** Waves and surge during Hurricane Sandy (October 2012) inundated the beach and dunes, flooding coastal roads in Falmouth, Massachusetts, and Westerly, Rhode Island 2
- Figure 3.** Waves and surge during Hurricane Sandy (October 2012) eroded the dunes and caused structural failure in Westerly, Rhode Island..... 3
- Figure 4.** Sketch defining the relevant morphologic and hydrodynamic parameters in the storm impact scaling model of Sallenger (2000) (modified from Stockdon and others, 2009)..... 5
- Figure 5.** Examples of post-storm conditions after collision (Nags Head, North Carolina; Isabel, 2003), overwash (Santa Rosa Island, Florida; Ivan, 2004), and inundation (Dauphin Island, Alabama; Katrina, 2005)..... 6
- Figure 6.** Cross-shore profile of lidar gridded elevations indicating the locations of the dune crest (x_c, z_c), toe (x_t, z_t), shoreline (x_{sl}, z_{sl}), mean beach slope (β_m), mean high water (MHW), and high water line (HWL) 8
- Figure 7.** Cross-shore profile for a bluffed beach on Cape Cod, Massachusetts..... 9
- Figure 8.** Sea, Lake, and Overland Surges from Hurricanes (SLOSH) category 1 modeled surge maximum of the maximum (MOM) for the Providence/Boston basin 11
- Figure 9.** The Simulating WAVes Nearshore (SWAN) model computational grid in UTM coordinates for Zone 19N..... 14

Figure 10. Modeled significant wave height (H_s) and parameterized peak period (T_p) at the 20-meter isobath extending from Rhode Island to Maine for category 1-4 hurricanes.....	15
Figure 11. Significant wave height (H_s) and peak (T_p) wave periods observed at NOAA buoy 44007 southeast of Portland, Maine	16
Figure 12. Maximum shoreline water level (η_{98}) for a category 1 hurricane and raw and smoothed dune crest elevation (z_c) for a 1-kilometer alongshore section	18
Figure 13. Distributions of dune crest elevation (z_c), dune toe elevation (z_t), and mean beach slope (β_m) for the northeast Atlantic sandy coastlines.....	20
Figure 14. Mean dune crest elevation (μz_c) for 1-kilometer sections of northeast Atlantic coastline compared to the standard deviation (σz_c) in those sections.....	21
Figure 15. Distribution of dune crest (z_c) and dune toe (z_t) elevations for Rhode Island, Massachusetts, New Hampshire, and Maine.....	22
Figure 16. Dune crest (z_c) and dune toe (z_t) elevations and hurricane-induced mean (η_{50}) and maximum (η_{98}) shoreline water levels extending from Rhode Island to Maine	23
Figure 17. Distributions of mean beach slope (β_m) elevations for Rhode Island, Massachusetts, New Hampshire, and Maine.....	24
Figure 18. Probabilities of collision, overwash, and inundation during a category 1 hurricane for Rhode Island, Massachusetts, New Hampshire, and Maine.....	27

Tables

Table 1. Mean elevation of dune crest (z_c), dune toe (z_t), and mean beach slope (β_m) for the sandy beaches along the northeast Atlantic coast	33
Table 2. Mean input wind speed, significant wave height (H_s), wave period (T_p), modeled setup (η_{setup}), runup (η_{R2}), and storm surge (η_{surge}) for category 1–4 hurricanes	33
Table 3. Percentage of coast very likely ($p>0.9$) to experience erosion associated with collision, overwash, and inundation during category 1–4 hurricanes.....	34

Conversion Factors

SI to Inch/Pound

Multiply	By	To obtain
Length		
centimeter (cm)	0.3937	inch (in.)
millimeter (mm)	0.03937	inch (in.)
meter (m)	3.281	foot (ft)
kilometer (km)	0.6214	mile (mi)
kilometer (km)	0.5400	mile, nautical (nmi)
meter (m)	1.094	yard (yd)
Flow rate		
meter per second (m/s)	2.237	mile per hour (mi/h)

Vertical coordinate information is referenced to the North American Vertical Datum of 1988 (NAVD88).

Horizontal coordinate information is referenced to the North American Datum of 1983 (NAD83).

Abbreviations

CHARTS	Compact Hydrographic Airborne Rapid Total Survey
CRM	Coastal Relief Model
DEM	Digital Elevation Model
EAARL	Experimental Advanced Airborne Research Lidar
GPS	Global Positioning System
HWL	High Water Line
Hz	Hertz
IPCC	Intergovernmental Panel on Climate Change
Lidar	Light Detection and Ranging
MHW	Mean High Water
MOM	maximum of the maximum
NAD83	North American Datum of 1983
NAVD88	North American Vertical Datum of 1988
NGDC	National Geophysical Data Center
NGVD29	National Geodetic Vertical Datum of 1929
NHC	National Hurricane Center
NOAA	National Oceanic and Atmospheric Administration
RMS	root-mean-square

SLOSH	Sea, Lake, and Overland Surges from Hurricanes
SWAN	Simulating WAVes Nearshore
USACE	U.S. Army Corps of Engineers
USGS	U.S. Geological Survey
WIS	Wave Information Studies

National Assessment of Hurricane-Induced Coastal Erosion Hazards: Northeast Atlantic Coast

By Justin J. Birchler, Hilary F. Stockdon, Kara S. Doran, and David M. Thompson

1. Introduction

1.1 Impacts of Hurricanes on Coastal Communities

Beaches serve as a natural buffer between the ocean and inland communities, ecosystems, and natural resources. However, these dynamic environments move and change in response to winds, waves, and currents. During extreme storms, changes to beaches can be great, and the results are sometimes catastrophic. Lives may be lost, communities destroyed, and millions of dollars spent on rebuilding.

During storms, large waves may erode beaches, and high storm surge may shift the erosive force of the waves higher on the beach. In some cases, the combined effects of waves and surge may cause overwash (when waves and surge overtop the dune, transporting sand inland) or flooding. Buildings and infrastructure on or near a dune can be undermined during wave attack and subsequent erosion. Hurricanes Irene and Sandy made landfall along the Eastern United States in August 2011 and October 2012, respectively. Although these hurricanes made landfall south and west of the northeast Atlantic coast, waves from these storms caused severe erosion and undermining, destroying roads in some areas of the coast (for example Westport, Massachusetts, fig. 1).



Figure 1. Collapsed road in Westport, Massachusetts, as a result of erosion during Hurricane Irene (August 2011). (Photo credit: Massachusetts Coastal Storm Damage Assessment Team)

Waves overtopping a dune can transport water and sand inland, covering roads and blocking evacuation routes or impeding emergency relief (fig. 2). If storm surge inundates barrier island dunes, currents flowing across the island can create a breach, or a new inlet, completely severing evacuation routes.



Figure 2. Waves and surge during Hurricane Sandy (October 2012) inundated the beach and dunes, flooding coastal roads in Falmouth, Massachusetts (top), and Westerly, Rhode Island (bottom). (Photo credit: top, Buzzards Bay National Estuary Program; bottom, National Weather Service, Taunton, Massachusetts)

Extreme coastal changes caused by hurricanes may increase the vulnerability of communities both during a storm and to future storms. For example, when sand dunes are substantially eroded, inland structures are exposed to storm surge and waves (fig. 3). On barrier islands, absent or low dunes allow water to flow inland across the island, potentially increasing storm surge in the back bay, on the sound-side of the barrier, and on the mainland.



Figure 3. Waves and surge during Hurricane Sandy (October 2012) eroded the dunes and caused structural failure in Westerly, Rhode Island. (Photo credit: National Weather Service, Taunton, Massachusetts)

1.2 Prediction of Hurricane-Induced Coastal Erosion

Waves and surge accompanying hurricanes, tropical storms, and nor'easters may result in widespread beach and dune erosion and extensive overwash. A clear need exists to identify areas of our coastline that are likely to experience severe erosion during extreme storms. This information can be used to determine vulnerability levels and the associated risk of building houses or infrastructure on land that shifts and moves with each storm landfall.

Communities along the northeast Atlantic coast of the United States are not often affected by hurricanes, as landfall in this region is uncommon. The most recent hurricane to make landfall in the Northeast was Hurricane Bob in 1991. However, hurricanes and tropical storms that remain offshore can still have an impact on sandy beaches because of strong wind, storm surge, and waves directed toward the coast. Nor'easters, though usually weaker than hurricanes, are perhaps more important drivers of coastal erosion in this region as they are more frequent and, because of their slow movement, can affect the coast for days rather than hours (Zhang and others, 2001).

A decade of research within the U.S. Geological Survey (USGS) National Assessment of Coastal Change Hazards project on storm-driven coastal change hazards has provided the data and modeling capabilities to produce the first regional assessment of the vulnerability of coastlines to extreme erosion during hurricane landfall. Vulnerability is defined in terms of the probability for coastal change, predicted using a USGS-developed storm-impact scale that compares predicted elevations of hurricane-induced water levels to measured elevations of coastal topography (Sallenger, 2000). The coastal morphology in the northeast Atlantic region includes both rocky coasts and sandy beaches. Rocky coasts tend to be much more resilient to storms and our formulations are specifically designed for sandy beaches; therefore, the focus in this report is on the vulnerability of open-coast sandy beaches on the U.S. northeast Atlantic shoreline.

1.3 Storm-Impact Scaling Model

During a storm, the combined effects of (1) the astronomical tide, (2) storm surge, and (3) wave runup (both setup, η_{setup} , and swash, S) move the erosive forces of the storm higher on the beach than during typical wave conditions. The total elevation of these three parameters defines two key metrics that characterize the nearshore hydrodynamic forcing of a storm: (1) the extreme high water level attained during a storm, defined here as the 98-percent exceedance level (η_{98}), and (2) the storm-induced mean water level (η_{50}), defined by only storm surge, tide, and wave setup.

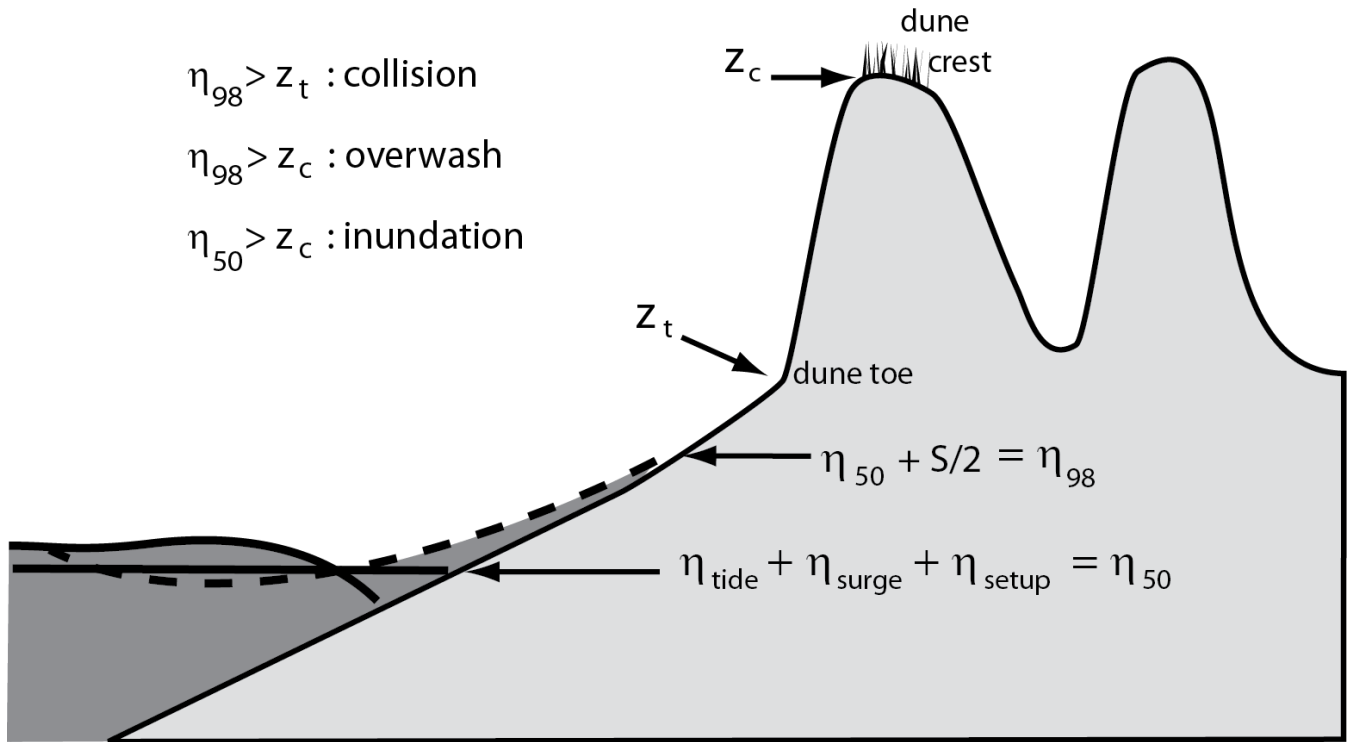


Figure 4. Sketch defining the relevant morphologic and hydrodynamic parameters in the storm impact scaling model of Sallenger (2000) (modified from Stockdon and others, 2009).

Water-level elevations are compared to the elevation of the toe (z_t) and crest (z_c) of the most seaward sand dune that defines the landward limits of the beach system and represent the first-line defense of a barrier island to an approaching storm. Using these parameters, four storm-impact regimes, or thresholds for coastal change, have been defined to provide a framework for examining the general types and relative magnitudes of coastal change that are likely to occur during hurricanes (fig. 4) (Sallenger, 2000; Stockdon and others, 2007a). These storm-impact regimes are:

- *swash* ($\eta_{98} < z_t$)
- *collision* ($\eta_{98} > z_t$)
- *overwash* ($\eta_{98} > z_c$)
- *inundation* ($\eta_{50} > z_c$)

(Note: Following Plant and Stockdon (2012), our nomenclature differs from Sallenger (2000) to emphasize probabilistic definition of water levels and to clearly distinguish both the horizontal and vertical components of dune morphology.)



Figure 5. Examples of post-storm conditions after collision (Nags Head, North Carolina; Isabel, 2003), overwash (Santa Rosa Island, Florida; Ivan, 2004), and inundation (Dauphin Island, Alabama; Katrina, 2005).

The *swash* regime represents a range of relatively calm weather conditions, where water levels are confined to areas seaward of the dune base. Sand that is eroded from the beach during more energetic periods is generally transported offshore and may be returned to the beach during more quiescent conditions. The erosion and recovery cycle can occur over a time span on the order of weeks. When waves reach the base of the dune (*collision* regime), the front of the dune is expected to erode (fig. 5, left). Again, sand is transported seaward and then re-deposited on the beach or sandbar. In this case, the beach is likely to recover in the weeks and months following the storm. However, because aeolian processes are responsible for natural dune growth, recovery of the dune may take years. Some portion of the total sand transport is directed alongshore, but the gradients are assumed to be small for purposes of these assessments.

In extreme cases, such as during stronger storms and for relatively lower dunes, waves and surge may exceed the dune crest elevation (*overwash* regime). Under these conditions, waves transport sand landward from the beach and dune (fig. 5, center). Impacts may be more long-lasting in this regime as sand is deposited inland, making it unavailable for natural recovery following a storm. During the *inundation* regime (fig. 5, right), storm-induced mean water levels exceed the elevation of the crest of the primary dune or berm. Some of the most extreme coastal changes on barrier islands occur within this regime; the beach system (dune crest and beach) is completely submerged, and net landward transport of sediment is likely to occur (Sallenger, 2000). Typically, larger magnitudes of shoreline retreat and beach erosion will occur when the dune is inundated as a result of sand transport occurring under all storm-scale regimes (Stockdon and others, 2007a). On narrow barrier islands, inundation allows strong currents to cross the island and focus erosion where dunes are low, thus carving breaches.

The predictive accuracy of the storm-impact scaling model was tested by hindcasting the likely impacts of Hurricanes Bonnie (1998) and Floyd (1999) (Stockdon and others, 2007a) and of Hurricane Ivan (2004) (Stockdon and others, 2007b) and comparing these with observed morphologic changes. For Hurricane Bonnie, the overall hindcast accuracy of the model in predicting one of the four regime types was 51 percent, while the accuracy for Floyd was a slightly improved 58 percent. For Hurricane Ivan, the overall hindcast accuracy of the model in predicting one of the four regime types was 68 percent. The accuracy of the model varied among regimes and was highest for the overwash conditions. Underprediction of the actual storm response was more likely than overprediction. Prediction errors were likely due to profile evolution of the low-lying barriers during the storm. Waves and surge may erode the beach and dune for several tidal cycles before the storm makes landfall. If substantial dune erosion

occurs, the beach will be more vulnerable to overwash and inundation than the initial, pre-storm morphology indicated.

Skillful hindcast results (Stockdon and others 2007a, 2007b) indicated the model was robust enough to be applied in real time for landfalling hurricanes (Plant and others, 2010; see also <http://coastal.er.usgs.gov/hurricanes/sandy/coastal-change/>). Using pre-storm measurements of dune elevations and real-time forecasts of storm surge and wave conditions in conjunction with the storm-impact scaling model, the USGS routinely reports the likelihood of beaches experiencing coastal change associated with collision, overwash, and inundation. These analyses are posted online (<http://coastal.er.usgs.gov/hurricanes/>) and revised with updated hydrodynamic forecasts as a storm approaches landfall.

Using a methodology similar to the real-time forecasts, this report quantifies the likely impact of hypothetical hurricane landfalls on the U.S. northeast Atlantic coastline, including Rhode Island, Massachusetts, New Hampshire and Maine. The probabilities of hurricane-induced coastal change are used to define the vulnerability of this region to extreme erosion from waves and storm surge associated with category 1–4 hurricanes. This report, along with similar analyses for the Gulf of Mexico shorelines (Stockdon and others, 2012), southeast Atlantic shorelines (Stockdon and others, 2013), and mid-Atlantic shorelines (Doran and others, 2013), forms the basis of a national assessment of storm-induced coastal erosion hazards.

2. Methods

In order to use the storm-impact scaling model for a large-scale assessment of the potential for coastal change during future hurricane landfall, accurate estimates of (1) the dune parameters and (2) the expected hurricane-induced water level for hypothetical storms are needed. Well-documented models of storm surge have been used to estimate worst-case scenarios of water-level elevations for category 1–4 hurricanes and can be used directly by our modeling approach. Simulations of corresponding wave conditions for category 1–4 hurricane landfalls are more challenging, but given simplifying assumptions it is possible to determine worst-case scenario wave heights for each category. Numerical simulations of storm surge and wave heights support application of our approach to large stretches of coast. Light detection and ranging (lidar) topographic surveying has made it possible to accurately measure dune elevations along extended (hundreds of kilometers) lengths of coastline. The combination of high-resolution measurements and advanced hydrodynamic modeling makes it possible to estimate probabilities of hurricane-induced coastal change and to identify coastal erosion vulnerability at a national scale.

2.1 Lidar-Derived Beach Morphology

The morphology of the beaches and dunes was mapped using airborne lidar topographic surveys conducted in 2010 by the U.S. Army Corps of Engineers (USACE) Compact Hydrographic Airborne Rapid Total Survey (CHARTS). The combination of laser-based ranging with inertial and global positioning system (GPS)-based navigation provides an efficient method for collecting high-resolution data of sub-aerial topography with sufficient accuracy (root-mean-square (RMS) vertical accuracy = 15 centimeters, cm; horizontal accuracy = 1–1.5 meters, m) to resolve the spatial details of sand-dune elevation and position (Sallenger and others, 2003). Three-dimensional lidar data were gridded using a fixed-scale interpolator (Plant and others, 2002), which allows for variability in cross-shore and

alongshore resolution, here, 2.5 m and 10 m, respectively. In addition to a gridded topographic surface, this method produces a corresponding grid of the RMS error, which provides a measure of noise in the data. A Hanning filter with a width equal to two times the grid resolution was chosen to minimize noise in the data associated with vegetation, alongshore variability, and other error sources while preserving distinct morphology. Analysis of cross-shore profiles of gridded data allows for automated extraction of dune crest (z_c) and toe (z_t), as well as shoreline position (x_{sl}) and beach slope (β_m), at a regular alongshore interval of, here, 10 m (fig. 6). These features are ultimately used to estimate wave runup and the corresponding storm-response regimes, as well as to quantify actual morphologic changes before and after storms. Detailed descriptions of the algorithm used to extract shoreline position, dune crest and toe, and beach slope can be found in the first report of this series, “National Assessment of Hurricane-Induced Coastal Erosion Hazards: Gulf of Mexico” (Stockdon and others, 2012), and references contained therein.

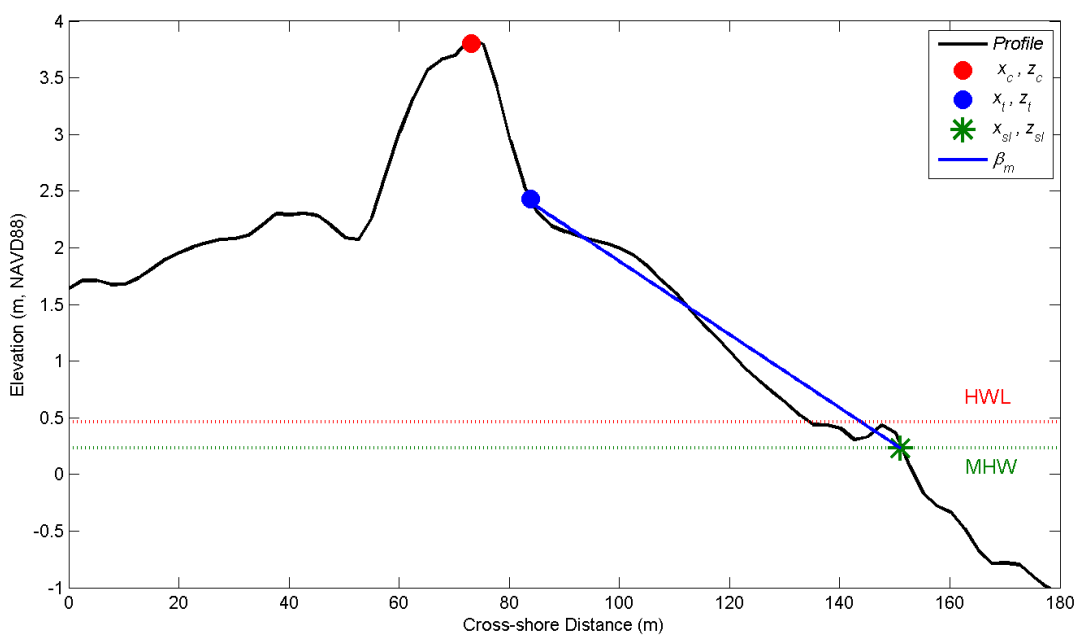


Figure 6. Cross-shore profile of lidar gridded elevations indicating the locations of the dune crest (x_c, z_c), toe (x_t, z_t), shoreline (x_{sl}, z_{sl}), mean beach slope (β_m), mean high water (MHW), and high water line (HWL). Abbreviation: m, meter.

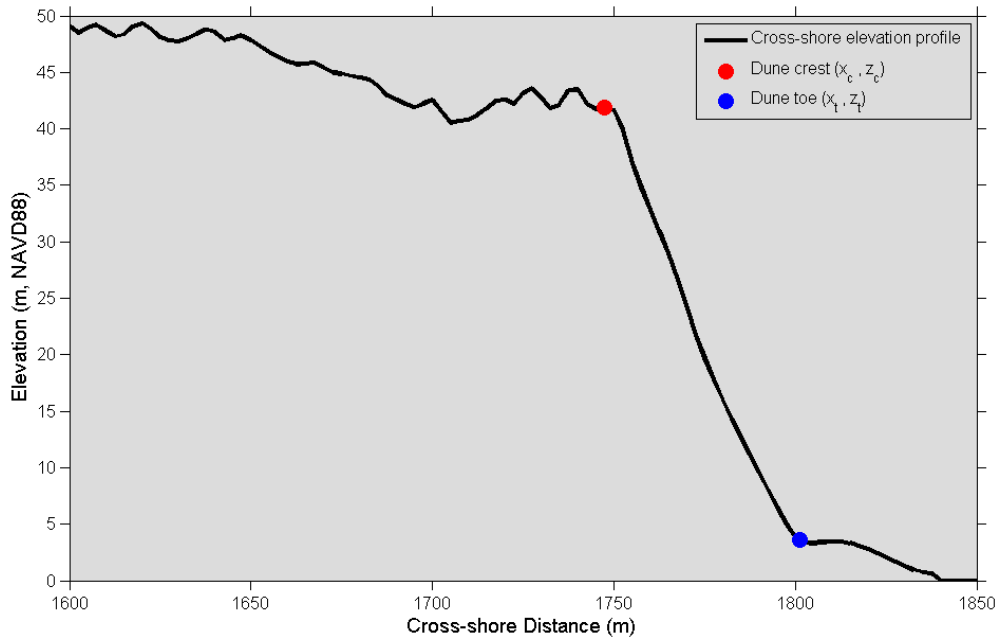


Figure 7. Cross-shore profile for a bluffed beach on Cape Cod, Massachusetts. The black line represents the lidar-derived elevation. Abbreviation: m, meter.

Where dune-backed beaches were not present, alternate methods were used to extract z_c . Aerial imagery was used to identify areas with rocky coastlines. In these regions, dune parameters that were mistakenly selected by the automated method were rejected and are not included in subsequent analyses. Bluffed coasts, composed of consolidated sands, were easily identified using the cross-shore elevation profiles because the bluff crest height is much greater than that of a typical sand dune (fig. 7). Bluff crests sometimes exceeded 40 m in elevation. Where there was a dune seaward of the bluff, typical dune parameters were selected; otherwise, the bluff crest was chosen as the dune crest.

2.2 Hurricane-Induced Water Levels

During a hurricane, water levels at the shoreline include the combined effects of tide, storm surge, and local wave energy. Predictions of coastal change during hurricanes require estimates of both the mean and extreme water levels that can be expected for each category. The mean hurricane-induced water level, η_{50} , is defined as

$$\eta_{50} = \eta_{tide} + \eta_{surge} + \eta_{setup} \quad (1)$$

where η_{tide} is the astronomical tide level, η_{surge} is storm surge, and η_{setup} is wave setup, the super-elevation of the water surface at the shoreline due to wave breaking. The extreme water level (η_{98}) attained during the storm includes wave swash, the time-varying component of wave energy on the beach, and is defined as

$$\eta_{98} = \eta_{50} + 1.1(S/2) \quad (2)$$

where S is the total swash excursion about the setup level and the 1.1 multiplier corrects for parameterization bias. It is important to note that both the mean and maximum water levels include a contribution from waves, which can increase water levels at the shoreline by the same magnitude as surge for category 1–3 hurricanes (Stockdon and others, 2007a).

2.2.1 Tide and Storm Surge

The predicted elevations of combined high tide and storm surge ($\eta_{tide} + \eta_{surge}$) for category 1–4 hurricanes were extracted from the National Oceanic and Atmospheric Administration (NOAA) SLOSH (Sea, Lake, and Overland Surges from Hurricanes) model, which has been used by NOAA for inundation risk studies and operational storm surge forecasting. The numerical model is based on linearized, depth-integrated equations of motion and continuity (Jarvinen and Lawrence, 1985). Storm surge is modeled by simulating the conditions of each category storm approaching the coast from different angles and at varying speeds. Changes in maximum surge elevations are forced by time-varying wind-stress and pressure-gradients that depend on the hurricane location, minimum pressure, and the radius of maximum winds (Jarvinen and Lawrence, 1985).

Storm surge levels ($\eta_{tide} + \eta_{surge}$) are simulated for each storm category in each of three model domains (New York, Providence/Boston, Penobscot Bay) subdividing the northeast Atlantic region. These simulations represent the peak water levels in each domain forced by thousands of hypothetical storms of varying forward speed, size, and direction, under mean-higher-high water tide conditions. The SLOSH model does not simulate category 5 hurricanes north of the Pamlico Sound basin, so only categories 1–4 are included in this report. The maximum surge within each grid cell, or the maximum of the maximum (MOM), represents a worst-case, localized surge level that could occur for a nearby hurricane landfall (fig. 8). (Note that the MOM is a composite from many storms and does not represent water levels that would occur along the entire coast for a single storm.) The resulting spatial variations in maximum storm surge reflect local water depths, proximity to bays and rivers, and so on and are accurate to ± 20 percent of the calculated value (NOAA, 2007). Prediction errors in the SLOSH model can arise from differences between the parametric wind models, which force SLOSH, and the actual hurricane wind field (Houston and others, 1999) as well as discrepancies between the coarse model grid and the actual topography and bathymetry over which the storm will travel. Additional constraints were applied to address some practical implementation problems associated with our use of the MOMs and are described in detail in Stockdon and others (2012).

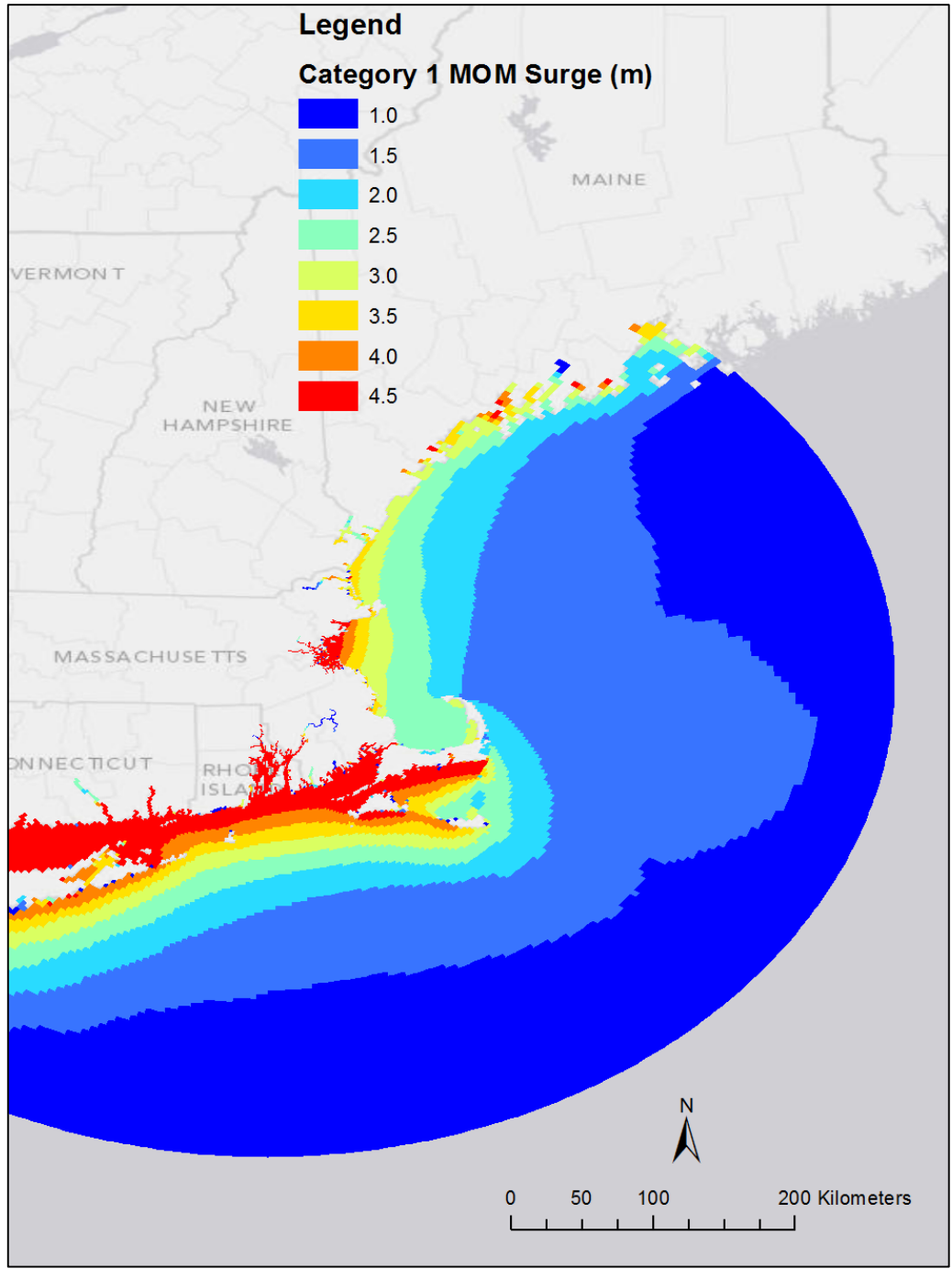


Figure 8. Sea, Lake, and Overland Surges from Hurricanes (SLOSH) category 1 modeled surge maximum of the maximum (MOM) for the Providence/Boston basin. Abbreviation: m, meter.

2.2.2 Wave Height and Period

Wave conditions vary spatially and temporally during hurricanes due to the same factors that cause variation in storm surge. Unfortunately, there is no equivalent of the MOMs that can be used to specify maximum wave height and period for category 1–4 hurricanes. Observations during hurricanes are incomplete because instrumented buoys tend to fail during conditions stronger than tropical storms. Long-term hindcasts of historical wave conditions (for example, USACE Wave Information Studies [WIS]) also underrepresent storm conditions. Therefore, wave conditions were estimated using the Simulating WAVes Nearshore (SWAN) model, a spectral wave model that resolves random, short-crested, wind-generated waves varying in time and space (Holthuijsen and others, 1993).

One approach to calculating storm-wave parameters would be to simulate individual idealized hurricanes using SWAN, much like was done with SLOSH in order to build a MOM-consistent dataset. However, an attempt to cover the entire coastline with idealized hurricane tracks and include a sufficient sampling of storm parameter space (wind speed, radius of maximum winds, forward speed, and so on) would require a massive computational effort. Furthermore, because we require wave information at a specific shallow water depth (20 m), the height of hurricane waves will tend to be limited by dissipation due to breaking, white-capping, and friction. Consequently, the sensitivity of parameterized shoreline water levels to wave parameter errors is expected to be limited as well.

Therefore, we apply a simple approach of generating stationary waves (in time) using SWAN for the maximum wind speed that defines each hurricane category over the entire mid- and north Atlantic basin. For determination of the contribution of waves to the total hurricane-induced water levels, the maximum wave-height value from an ensemble of simulations of the maximum wind speed was selected as the representative value for each category, very similar to the MOM product from the SLOSH model. As with the MOMs, these results do not represent an individual storm but rather a composite, worst-case estimate at each location from many storm scenarios.

For our analysis, SWAN version 40.85 was used. The model was run in third-generation mode using the Westhuysen formulation for white-capping and Yan formulation for wind input (GEN3 WESTH). Bottom friction was included using default values, and all other model parameters were left as default. The resolution of the SWAN computational grid was 1.5 kilometers (km) x 1.5 km (fig. 9). Bathymetry was interpolated from the National Geophysical Data Center (NGDC) Coastal Relief Model (CRM). SWAN was run 24 times for each wind speed, with direction varying from 0° to 345° at 15° increments. For each wind speed, the model results from the 24 wind direction runs were combined into a single grid by retaining the wave parameters from the wind direction that generated the largest significant wave height, H_s in each grid cell.

Simulated H_s at the 20-m isobaths for category 1–4 hurricanes varied along the northeast Atlantic coast (fig. 10). The resulting maximum wave heights at the 20-m isobaths for a category 1 hurricane typically ranged from about 6 m to about 10 m. Along the northern end of Cape Cod, Massachusetts, wave height reached 13 m for category 4 hurricane conditions due to a narrow continental shelf. To put these model results in context, we compared the modeled wave heights to the observed wave heights measured over a 32-year period from 1982 to 2013 at NOAA buoy 44007 (see http://www.ndbc.noaa.gov/station_page.php?station=44007) located at 24-m water depth, 17 km southeast of Portland, Maine. Annual maximum wave heights between 6 and 8 m typically were observed at this relatively shallow location. The largest wave heights recorded during this period were approximately 10 m, suggesting the simulated wave heights are representative of maximum possible wave heights during hurricane conditions.

The swash parameterization requires estimates of peak period, which were not reliably modeled owing to our simplified wind field. Consistent peak-period estimates were obtained from an analysis of 32 years of NOAA National Data Buoy Center data for shallow-water buoy 44007 operating in the north Atlantic. The analysis yielded a parameterized relation between significant wave height obtained from the SWAN model and peak wave periods (fig. 11).

$$T_p = b_0 + b_1 * H_s + b_2 * H_s^2, \quad (3)$$

where T_p is peak wave period and H_s is significant wave height. Data from the buoy in a water depth of 24 m was used in a linear regression to estimate the model coefficients, b_n , resulting in

$$b_0 = 6.6201 (\pm 0.0447)$$

$$b_1 = 0.9211 (\pm 0.0325)$$

$$b_2 = -0.0269 (\pm 0.0049)$$

This parameterization was used to compute peak wave periods for each hurricane category that were consistent with north Atlantic observations, using the simulated significant wave heights as input.

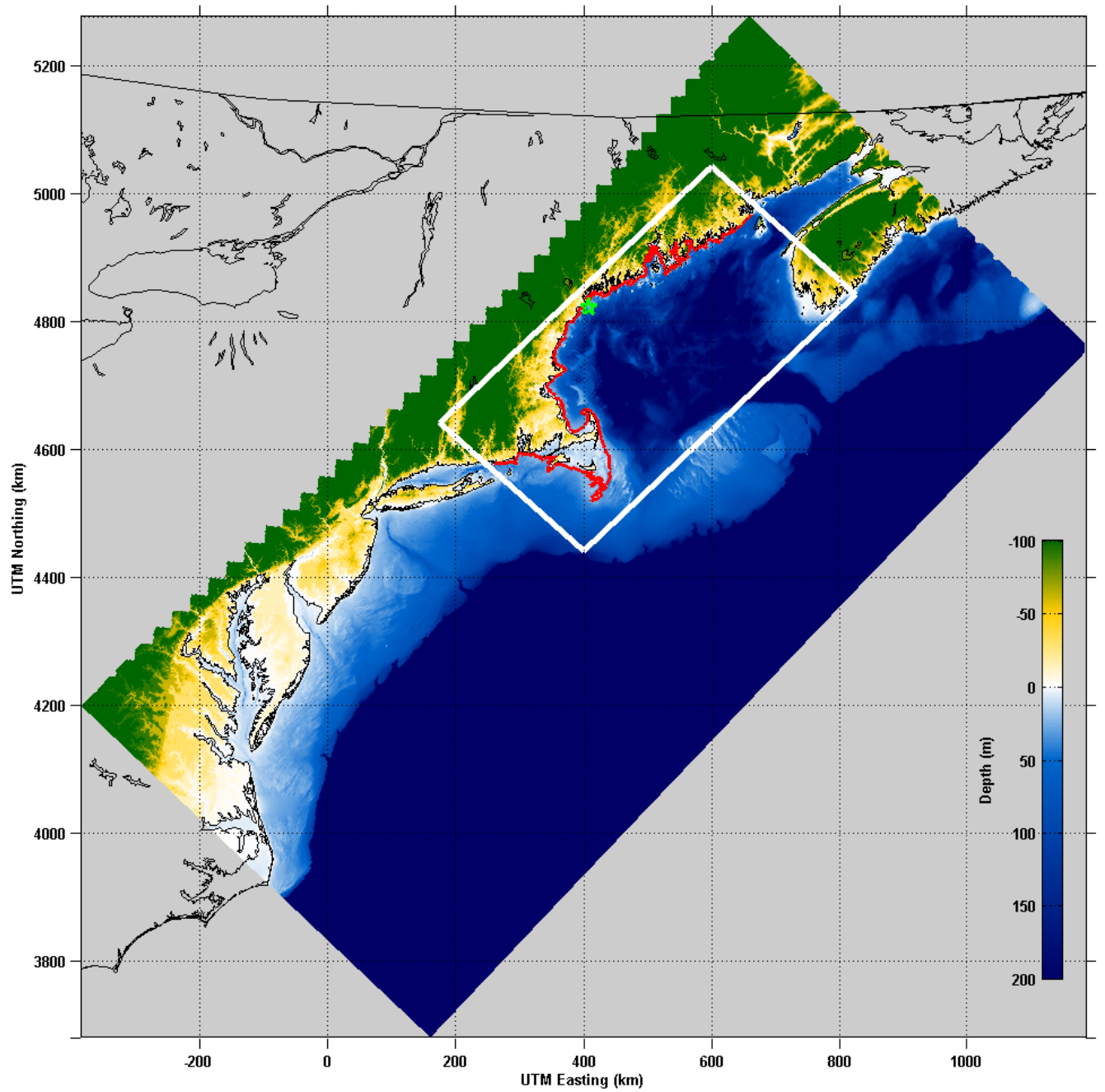


Figure 9. The Simulating WAVes Nearshore (SWAN) model computational grid in UTM coordinates for Zone 19N. Grid resolution is 1.5 kilometers. The study area is denoted by the white box and the 20-meter isobath along the study area is shown in red. The location of NOAA buoy 44007 is denoted by the green star. Abbreviation: m, meter.

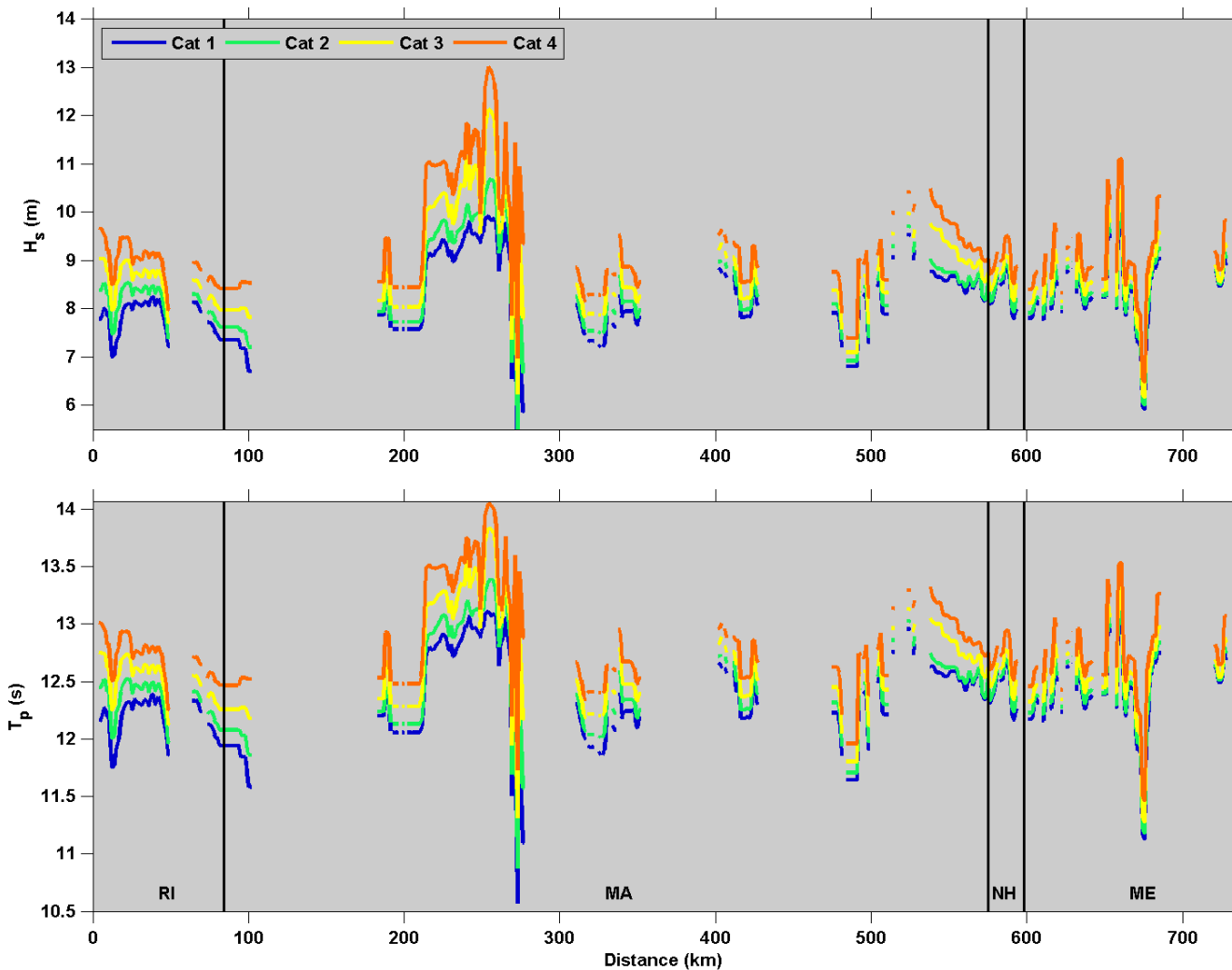


Figure 10. Modeled significant wave height (H_s , top) and parameterized peak period (T_p , bottom) at the 20-meter isobath extending from Rhode Island (left) to Maine (right) for category 1-4 hurricanes. State boundaries are indicated by vertical lines: RI, Rhode Island; MA, Massachusetts; NH, New Hampshire; ME, Maine. Breaks in the data indicate the absence of an open-coast beach; no wave parameters were calculated for these locations. Abbreviations: m, meter; km, kilometer; s, second.

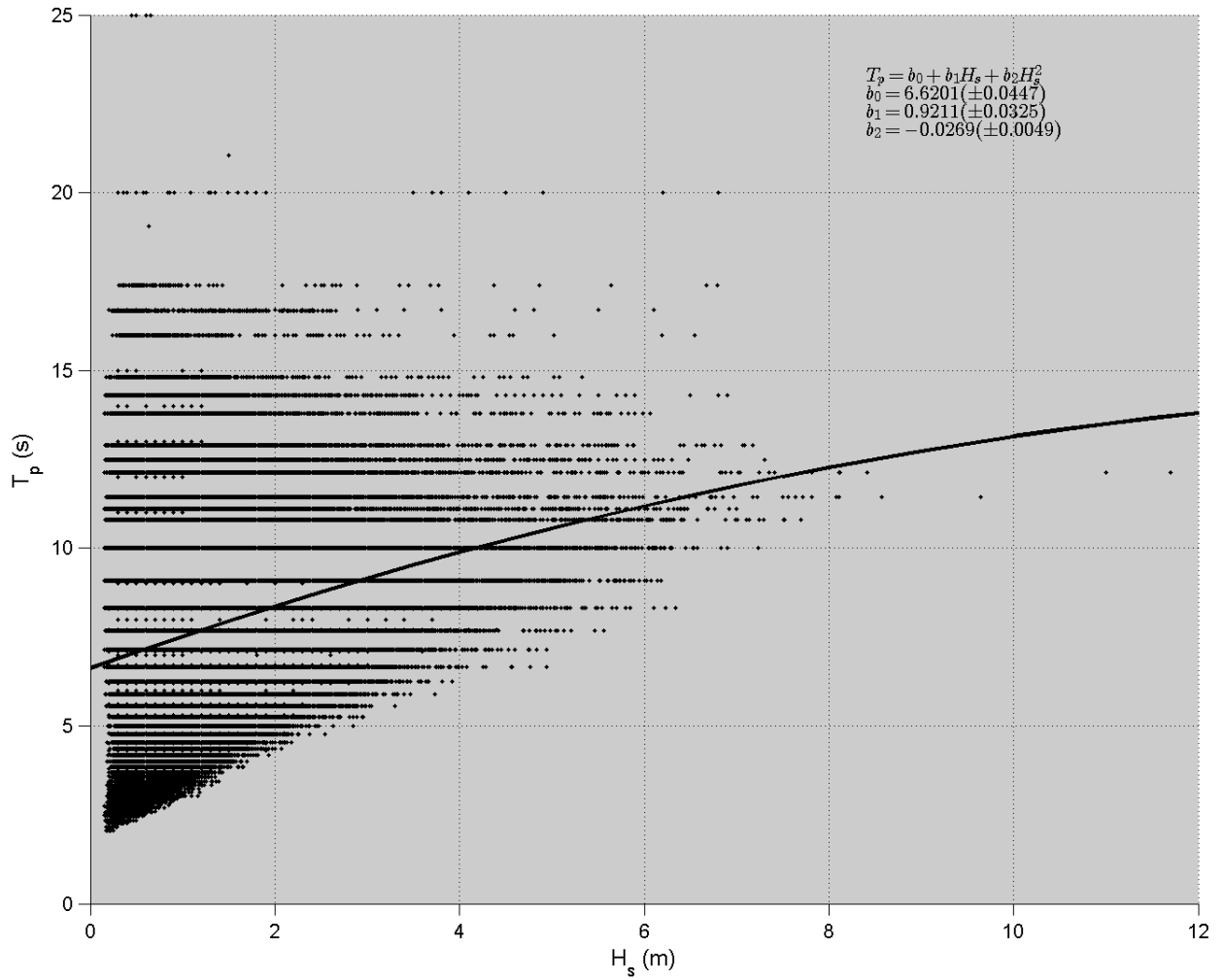


Figure 11. Significant wave height (H_s) and peak (T_p) wave periods observed at NOAA buoy 44007 southeast of Portland, Maine. The curve represents the weighted regression that is based on the buoy data. Abbreviations: m, meter; s, second.

2.2.3 Wave Setup and Swash

Swash and setup, the wave-induced components of total shoreline water levels, are parameterized using modeled wave conditions and measured beach slope (Stockdon and others, 2006). Setup, required in the calculation of both mean (η_{50}) and extreme (η_{98}) hurricane-induced water levels, is parameterized as

$$\eta_{setup} = 0.35\beta_m (H_0 L_0)^{1/2} \quad (4)$$

where $L_0 = gT_p^2/2\pi$ is the deep water wave length, and H_0 is the deep water wave height. Wave swash, S , is the time-varying component of water levels at the shoreline and part of the calculation of extreme (η_{98}) hurricane-induced water levels and is parameterized as

$$S = \left[H_0 L_0 (0.563 \beta_m^2 + 0.005) \right]^{1/2}. \quad (5)$$

Combining equations (4) and (5) with modeled η_{tide} and η_{surge} provided estimates of hurricane-induced mean and maximum water levels (equations 1 and 2).

2.3 Probability of Coastal Change

Probabilities of coastal change are based on estimating the likelihood that the beach system will experience erosion and deposition patterns consistent with the collision, overwash, or inundation regimes. Uncertainties that were incorporated in the probability estimates arise from that associated with measurements of topographic elevation (for example, lidar positional and interpolation uncertainties) and that associated with predicting wave runup elevations.

The probabilities of collision, overwash, and inundation were calculated using distributions of morphologic and hydrodynamic parameters extracted from 1-km sections of coast. Hydrodynamic and morphologic data were co-located alongshore using a common reference line (the 20-year high water line (HWL) shoreline (Ruggiero and List, 2009)). Morphologic features, z_c , z_t , and β_m , were interpolated to the reference line and smoothed using a Hanning window with a full width of 2 km. Each interpolated, smoothed value of (x_c, z_c) , (x_t, z_t) , and β_m was assigned a RMS error calculated from the scatter of the data in the smoothing window (fig. 12, top). The variables were represented with a normal distribution of values at the location of each 1-km section of coast using the interpolated value as the mean and the RMS error as the standard deviation (fig. 12, bottom). This analysis produced mean and standard deviations for both the hydrodynamic and the morphologic variables.

Using the statistical distribution of the input values at each alongshore location, the probability, p , that the total water level exceeds the dune crest or toe elevation threshold for a particular storm regime is calculated from the normal cumulative distribution function

$$p = \frac{1}{\sigma\sqrt{2\pi}} \int_0^{\infty} e^{-\frac{(t-\mu)^2}{2\sigma^2}} dt \quad (6)$$

where μ is the mean difference between either the mean (inundation) or extreme (collision, overwash) water levels and either the dune toe (collision) or dune crest (overwash, inundation). The variance of the difference, σ^2 , is the sum of the variances of the inputs. Thus, the probabilities of each storm-impact regime are calculated as:

- Collision: $p_c = \text{probability} ([\eta_{98} - z_t] > 0)$
- Overwash: $p_o = \text{probability} ([\eta_{98} - z_c] > 0)$
- Inundation: $p_i = \text{probability} ([\eta_{50} - z_c] > 0)$

For example, figure 12 shows the cumulative distribution of $(\eta_{98} - z_c)$ for a 1-km section of coast for a category 1 hurricane. The probability that this value exceeds zero defines the likelihood that overwash will occur at this location.

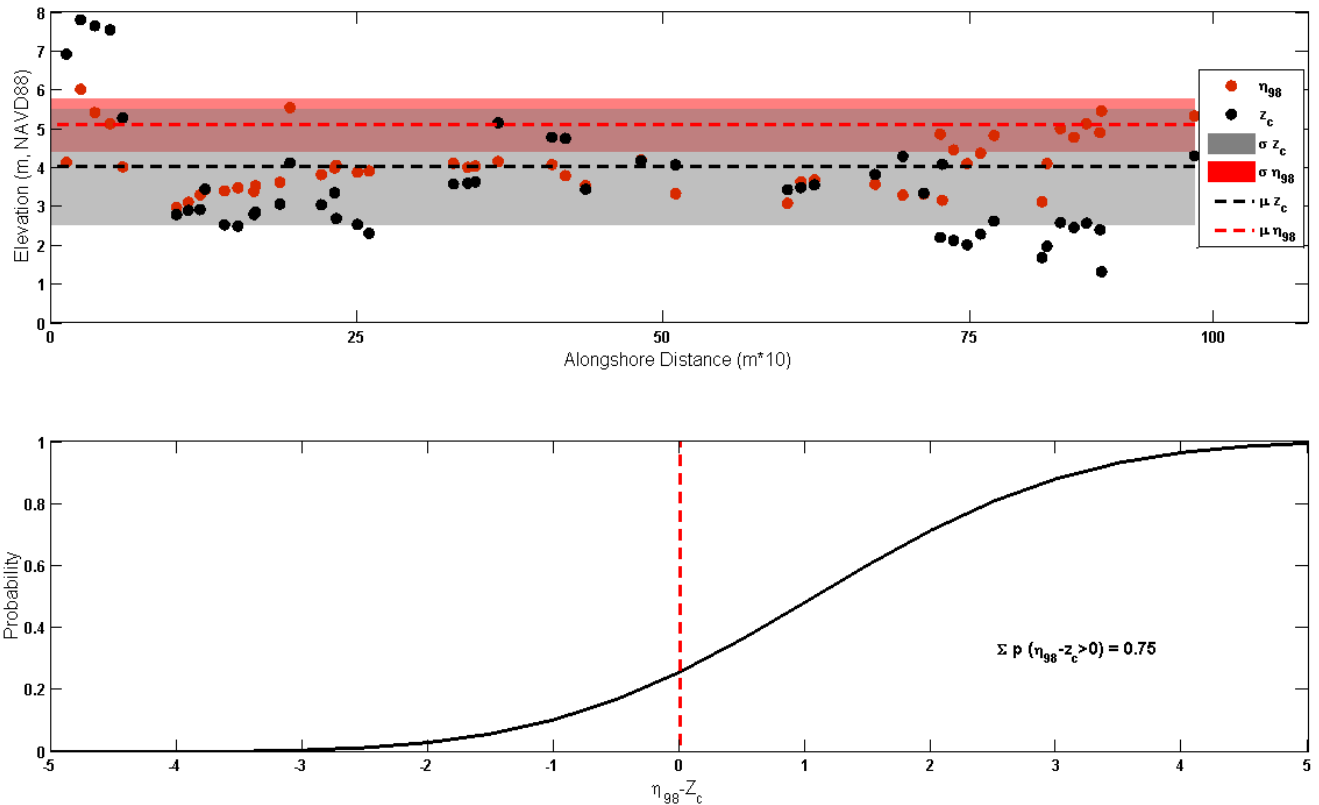


Figure 12. Maximum shoreline water level (η_{98}) for a category 1 hurricane and raw and smoothed dune crest elevation (z_c) for a 1-kilometer alongshore section (top). Shaded areas indicate the RMS error for dune crest elevation and maximum water level (σz_c and $\sigma \eta_{98}$) about the mean value (μz_c and $\mu \eta_{98}$) within the section. Cumulative probability distribution, $p(\eta_{98} - z_c)$ where the sum of p over the range $(\eta_{98} - z_c) > 0$ defines the probability of overwash (bottom). Abbreviation: m, meter.

3. Results

3.1 Coastal Morphology

In addition to sandy beaches, the coastal morphology along the northeast Atlantic coast includes sand, gravel, and mixed sediment beaches, as well as bluff-backed beaches and rocky coast. (See Section 4.4 for a more detailed discussion of regional beach morphology.) For this study, rocky coasts were omitted from the analysis because the models do not apply.

Dune morphologies along the northeast Atlantic coast vary over both short and long (regional) spatial scales (table 1). On dune-backed beaches, crest elevations range from 2 to 13 m. The mean dune

crest elevation (not including bluff-backed coasts), μ_{z_c} , for sandy beaches in this region is 4.83 m, similar to that in the mid-Atlantic (4.39 m) but almost a meter higher than dunes along the southeast Atlantic coast. The standard deviation, σ , of dune crest elevation is 1.81 m (fig. 13, top), indicating that spatial variability is high enough that low elevations ($\mu - 2\sigma$) may be below the HWL, suggesting that the dunes could be impacted by regular wave conditions. (Along the northeast Atlantic coast, HWL elevation ranges from 0.80 to 4.10 m NAVD88; the mean elevation is 1.21 m from Rhode Island through Monomoy Island, Massachusetts, and 1.92 m from Chatham, Massachusetts through Maine.) Local spatial variability tends to scale with dune elevation; locations with higher mean elevations often exhibit greater spatial variability (fig. 14). Dune toe elevations are consistently low with less spatial variability (fig. 13, middle; $\mu_{z_t} = 2.64$ m; $\sigma_{z_c} = 0.83$ m) and similar magnitude to that observed in the southeast and mid-Atlantic regions, 2.26 m and 2.63 m, respectively.

The highest dunes (z_c in excess of 10 m, not including bluff-backed coasts) are located in Massachusetts at the northern end of Cape Cod (figs. 15–16); however, spatial variability is high here ($\mu_{z_c} = 5.19$ m; $\sigma_{z_c} = 2.17$ m). The lowest elevations are found in Rhode Island, where $\mu_{z_c} = 4.09$ m and $\sigma_{z_c} = 0.85$ m. In New Hampshire, the dune crest elevation exhibits a bimodal probability distribution (fig. 15). About 60 percent of the New Hampshire dune crests have an elevation near 4 m, while about 13 percent have an elevation near 7 m. The lower elevation dunes are present in areas where the dunes are disturbed by development, while the higher elevation dunes are present in less developed areas. Dune toe elevation in New Hampshire does not exhibit this same bimodal distribution pattern.

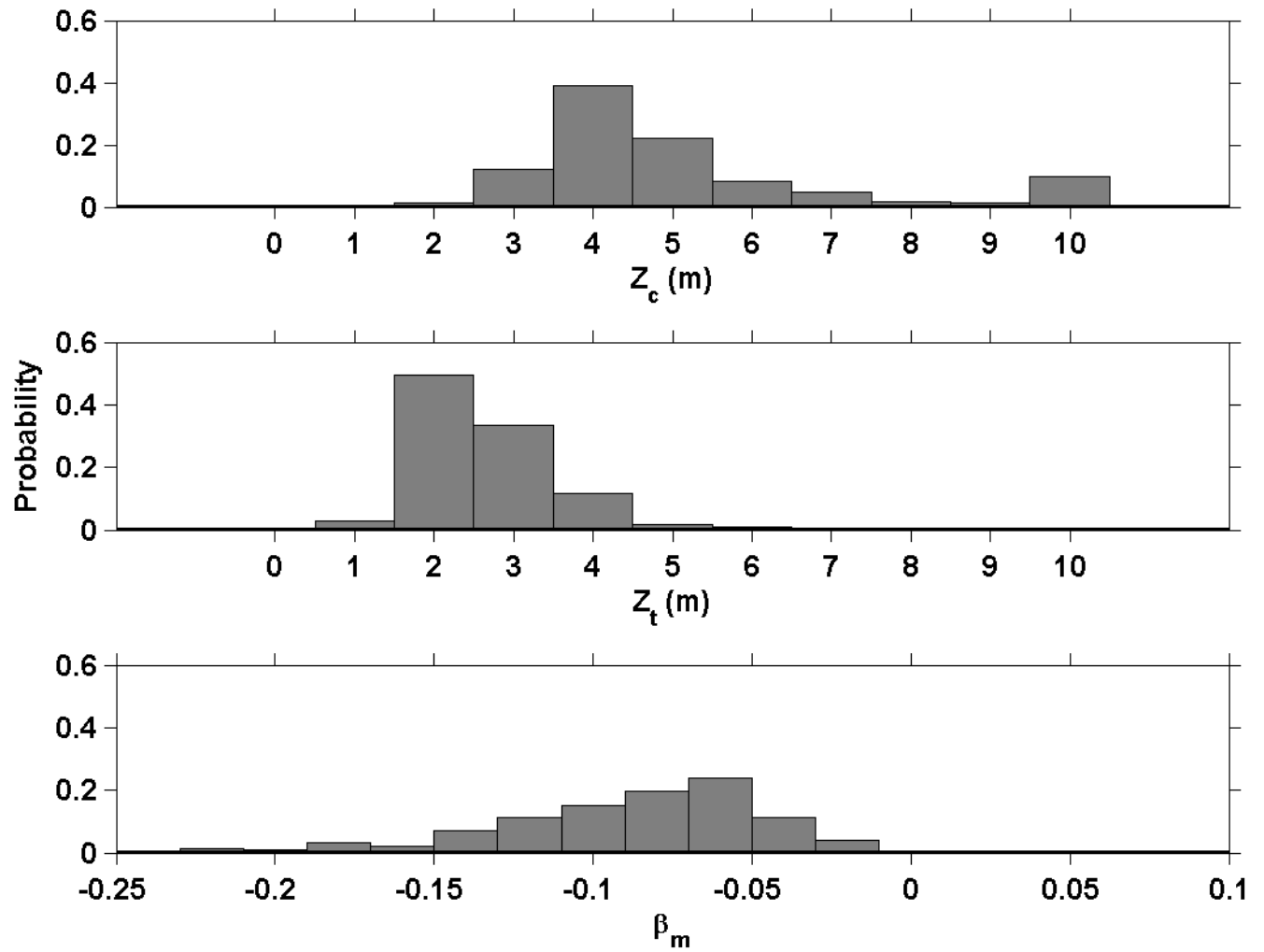


Figure 13. Distributions of dune crest elevation (z_c , top), dune toe elevation (z_t , middle), and mean beach slope (β_m , bottom) for the northeast Atlantic sandy coastlines. Abbreviation: m, meter.

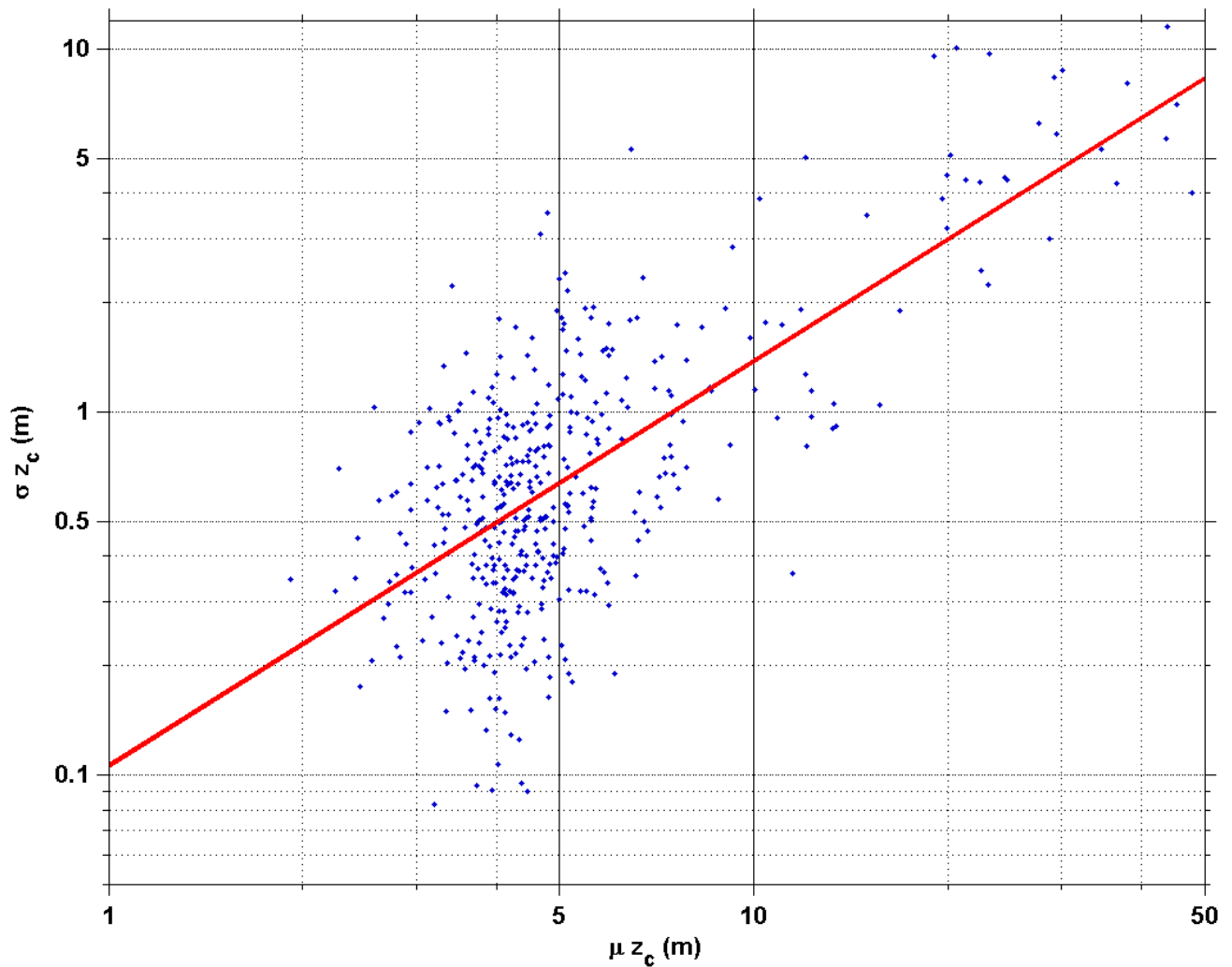


Figure 14. Mean dune crest elevation (μz_c) for 1-kilometer sections of northeast Atlantic coastline compared to the standard deviation (σz_c) in those sections. The red line indicates the best fit line between the two variables. $r^2 = 0.65$, $N = 442$. Note: Data are plotted on a log-log scale. Abbreviation: m, meter.

Part of the beach along Cape Cod, Massachusetts, is backed by sandy bluffs, which range in height from 10 to 50 m (see figure 15). Although it is extremely unlikely for the bluff crest to be subjected to overwash or inundation, the base of the bluff (dune toe) may be prone to erosion during extreme water levels. The location of the bluffed beaches in Massachusetts is shown in figure 16.

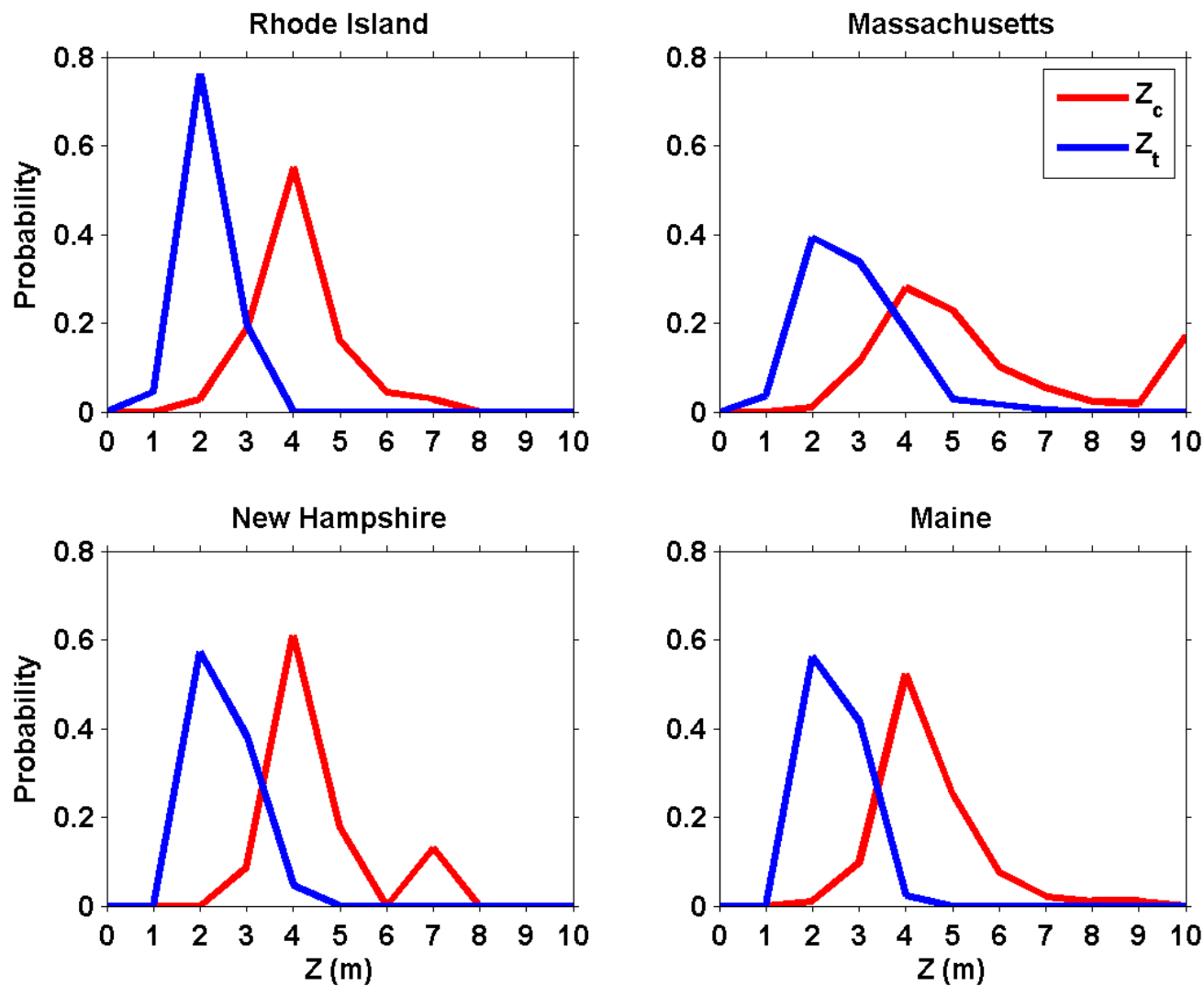


Figure 15. Distribution of dune crest (z_c) and dune toe (z_t) elevations for Rhode Island, Massachusetts, New Hampshire, and Maine. Abbreviation: m, meter.

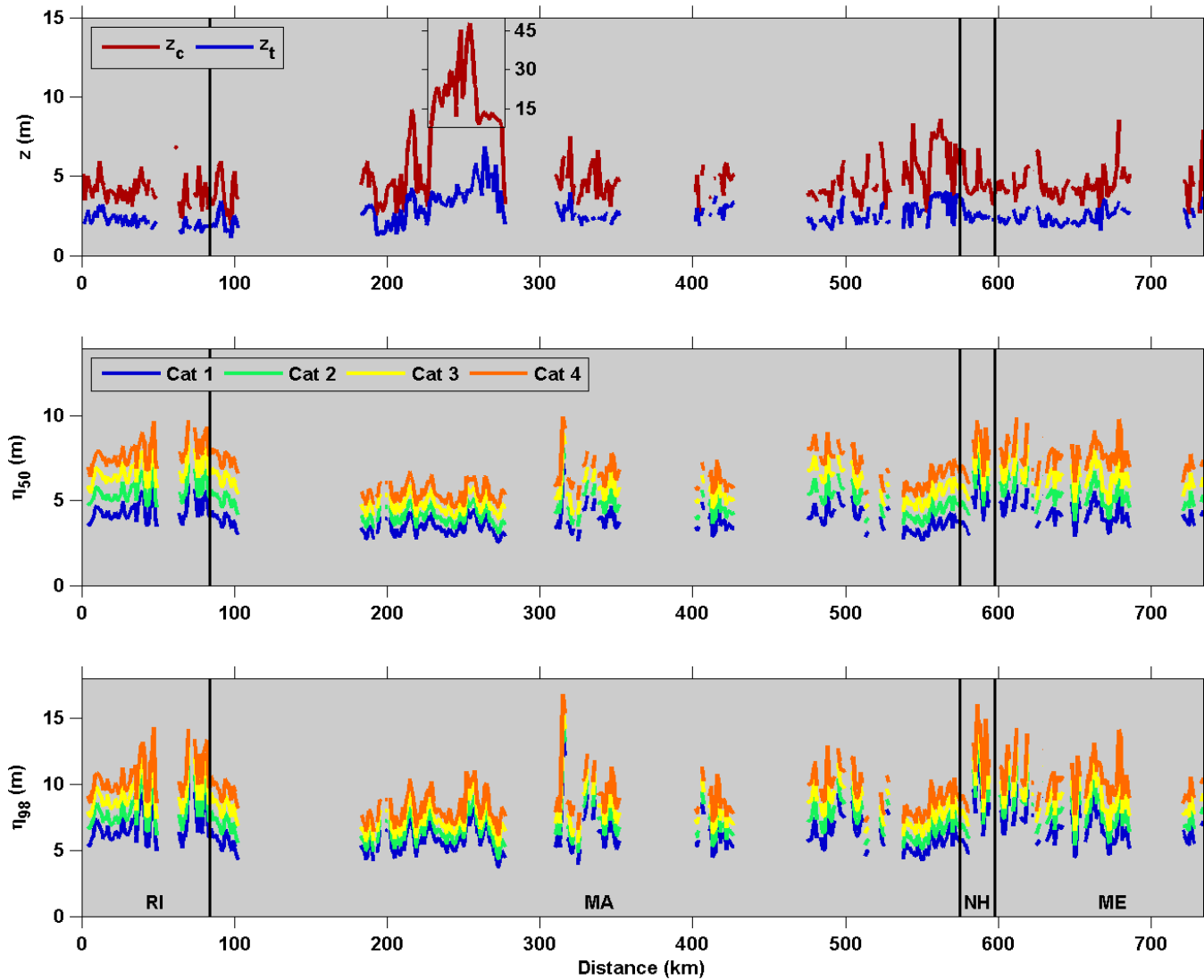


Figure 16. Dune crest (z_c , red line) and dune toe (z_t , blue line) elevations (top) and hurricane-induced mean (η_{50} ; middle) and maximum (η_{98} ; bottom) shoreline water levels extending from Rhode Island (left) to Maine (right). Area of bluff-backed beaches shown by inset dune crest axis. State boundaries are indicated by vertical lines. Breaks in the data indicate the absence of an open-coast beach; no dune or water level parameters were calculated for these locations. Abbreviation: m, meter; km, kilometer.

Although also spatially variable, mean beach slope along the northeast Atlantic coast is generally intermediate ($\mu\beta_m = 0.088$; $\sigma\beta_m = 0.044$, fig. 17), similar to the east coast of Florida ($\mu\beta_m = 0.082$; $\sigma\beta_m = 0.041$) but, in general, steeper than most beaches along the Gulf and mid- and southeast Atlantic coasts. The lowest slopes are located along the Massachusetts coast ($\mu\beta_m = 0.081$; $\sigma\beta_m = 0.041$). The steepest slopes are present along the New Hampshire coast ($\mu\beta_m = 0.131$); however, the standard deviation here was also greatest ($\sigma\beta_m = 0.073$), indicating a wide range of slopes. The steepest slopes in New Hampshire ($\beta_m > 0.15$) are due to a narrow beach, fronting revetment systems designed to protect coastal infrastructure.

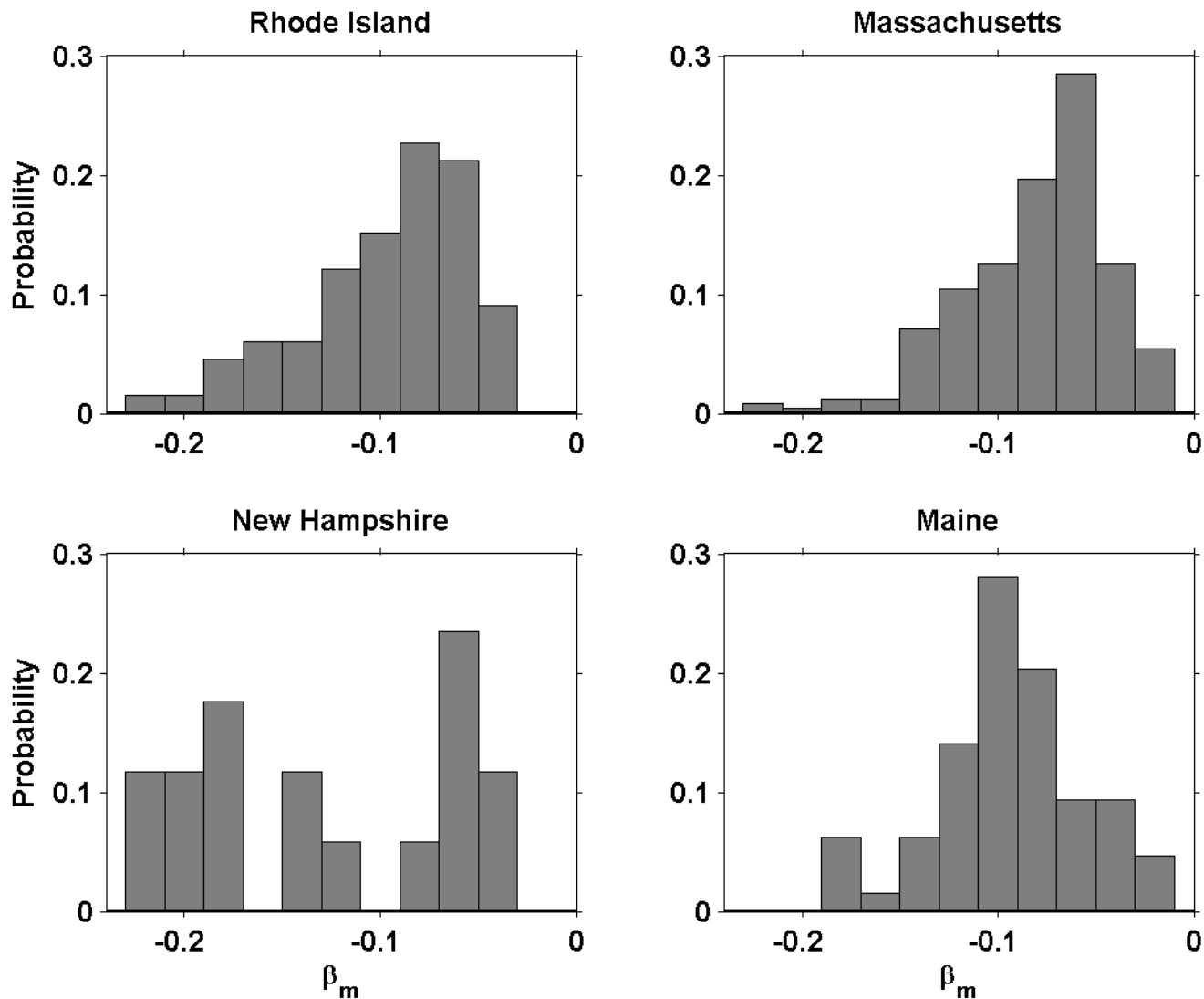


Figure 17. Distributions of mean beach slope (β_m) elevations for Rhode Island, Massachusetts, New Hampshire, and Maine.

3.2 Hurricane-Induced Water Levels

The variability of hurricane-induced water levels can be attributed to both hydrodynamics and beach morphology. Variability of H_s at $h = 20$ m within a single category, due to local bathymetry and dissipation from depth-limited breaking, white-capping, and bottom friction, leads to corresponding alongshore differences in η_{98} and η_{50} . The largest waves ($H_s = 13$ m) were located offshore of Cape Cod, Massachusetts, where the narrow shelf allows larger waves to make it to the nearshore (fig. 10; $x = 250$ km alongshore), because wave breaking and bottom dissipation act over very short distances before reaching the 20-m isobath. Large waves ($H_s = 11$ m) were also located along the narrow shelf near Cape Ann, Massachusetts, and Cape Elizabeth, Maine (fig. 10; $x = 520$ and 660 km alongshore). For the sandy beaches used in this analysis, however, variability of H_s generally is less than 1 m for a 10 km longshore extent within a single category, but variability ranges from 6 to 10 m across the entire northeast Atlantic coast for a category 1 storm, and standard deviation of H_s ranges from 0.80 m for a category 1 storm to 1.05 m for a category 4 storm (table 2).

For category 1–4 storm conditions, average runup along the northeast Atlantic coast is 3.8 to 4.1 m, 40–50 percent higher than that for the mid-Atlantic region where runup magnitudes range from 2.5 to 3 m. Regional variability in runup is due, in part, to spatial variations in beach slope, because the wave-driven components of shoreline water levels, η_{setup} and S , are dependent on input wave conditions and local slopes (equations 4 and 5). For similar input wave conditions, steeper beach slopes result in higher total runup elevations ($\eta_{R2} = 1.1[\eta_{setup} + S/2]$). In the northeast region, $\mu\beta_m$ is 85 percent higher than in other areas along the Atlantic coast. Within a region, smaller-scale variability can also be attributed to beach slope. For example, category 3 η_{R2} is 1.88 m higher for New Hampshire than for Massachusetts, despite the fact that mean wave height is 0.55 m lower. The higher wave runup is due to the steeper beach slope in New Hampshire ($\mu\beta_m = 0.131$) compared to that in Massachusetts ($\mu\beta_m = 0.081$).

The modeling exercise for the northeast Atlantic coast demonstrated the relative importance of waves with respect to storm surge. For a category 1 storm, wave-driven components represent 59 percent of the total hurricane-induced water levels; the remaining 41 percent is attributed to tides and surge (table 2). As the intensity of a storm increases, the relative contribution of wave-driven components decreases. In a category 4 hurricane, surge contributes 57 percent to the total water-level elevation while wave-driven components contribute the remaining 43 percent. Wave height does not continue to increase with increasing storm intensity because of dissipation through white-capping and breaking; however, surge continues to increase, approximately 1 m with each storm category.

3.3 Probability of Coastal Change

The probabilities of collision, overwash, and inundation indicate whether a specified coastal change regime is very likely (probability >90 percent), likely (>66 percent), about as likely as not (33 to 66 percent), unlikely (<33 percent), and very unlikely (<10 percent) given the local landfall of each hypothetical storm scenario. (Range descriptions are based on guidance from the Intergovernmental Panel on Climate Change (IPCC) (Cubasch and others, 2013).) Probabilities of coastal change for the lowest category hurricane show that beaches along the northeast Atlantic coast are vulnerable to dune erosion and overwash (fig. 18). For direct landfall of the lowest category hurricane, 96 percent of sandy beaches are very likely to experience dune erosion due to collision, and 54 percent of the coastal areas are vulnerable to overwash (table 3). Inundation of the beach and dune system is expected along 13 percent of the coastline, typically in areas in each state with fairly low elevation dunes (fig. 16). For a category 4 hurricane landfall, 82 percent of northeast Atlantic beaches are very likely to experience overwash and

associated beach and dune erosion (table 3), and the percentage of beaches that are very likely to be inundated increases to 69 percent.

The northeast Atlantic region is vulnerable to coastal change during extreme storms. The average dune elevation in this region is the highest along the Gulf and Atlantic coasts; however the maximum storm water levels are also the highest in this region. The Gulf of Mexico coast is slightly more vulnerable to coastal change during storms mainly because of low dune elevations. The southeast and mid-Atlantic coasts were slightly less vulnerable to coastal change because water levels were not as high as in the northeast, even though dune elevations were lower. For a category 4 storm, all coastal regions were likely to very likely to experience overwash and were likely to experience inundation.

Spatial variability exists over smaller spatial scales, on the order of kilometers, in areas with complex dune fields or extensive three-dimensional beach morphology. The mix of low and high dunes along the northeast Atlantic coast (fig. 16) leads to a complicated picture of hurricane-induced erosion hazards within each State and across the entire region. The smaller scale variability (alongshore spacing of 1 km), for a specific area, can be examined using interactive maps that are available online. The probability of each mode of coastal change for category 1–4 landfalls, as well as supporting morphology and water level data, are available online (<http://coastal.er.usgs.gov/hurricanes/erosionhazards/> and <http://marine.usgs.gov/coastalchangehazardsportal/>).

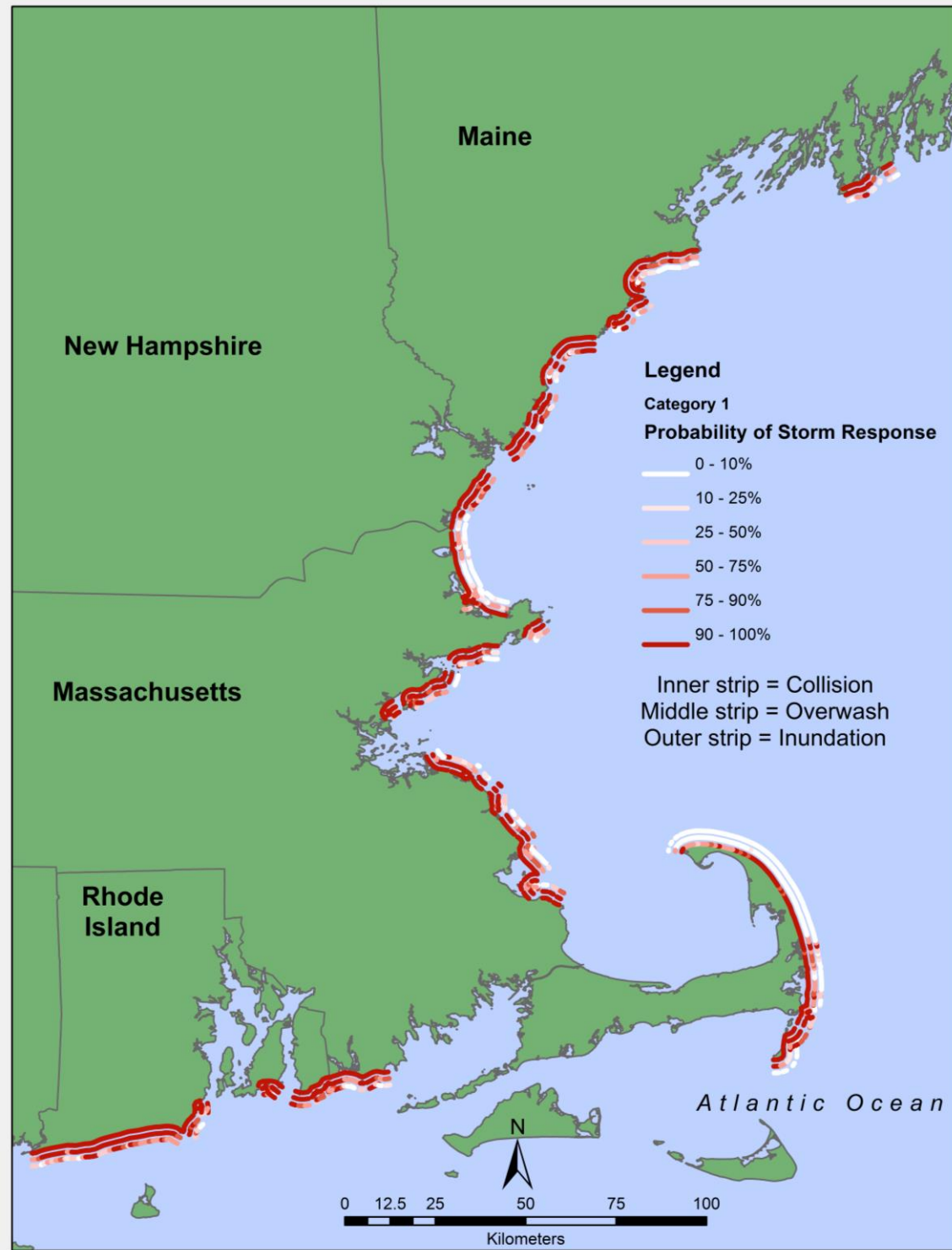


Figure 18. Probabilities of collision (inner strip), overwash (middle strip), and inundation (outer strip) during a category 1 hurricane for Rhode Island, Massachusetts, New Hampshire, and Maine. Where the dune is identified as a berm, the collision regime is undefined. Breaks in the data indicate the absence of an open-coast beach or lack of recent lidar data (e.g. Buzzards Bay, inner arm of Cape Cod, Nantucket Island).²⁸

4. Discussion

4.1 Validity of Assumptions

This analysis is based on an estimate of a worst-case scenario with respect to storm surge levels and wave heights associated with each hurricane category. The implied assumption is that each location along the coast experiences the right-front quadrant of the hurricane at landfall, which results in onshore-directed winds and the combined effects of both the circulation and the forward motion of the storm.

Waves and surge associated with an actual storm may be substantially different than model results. The SLOSH results are grouped by Saffir-Simpson categories, which are based on wind speeds. It is recognized that wind-based Saffir-Simpson categories are not always an accurate indicator of expected storm surge (Irish and others, 2008, 2009); however, they do provide a convenient way to represent the data based on storm intensity, allowing users to examine a range of conditions in a small number of scenarios. Real-time analysis of individual landfalling hurricanes includes more realistic updates of surge, tides, and waves (<http://coastal.er.usgs.gov/hurricanes/>).

This assessment also assumes that the existing lidar-surveyed topography is up to date and accurately and synchronously reflects dune and beach morphology. Substantial changes to beach and dune morphology between the survey date and dates of future hurricane landfall may affect the probabilities of coastal change. It is assumed that dune elevations change relatively slowly under non-storm conditions. Changes in beach slope, which will in turn affect the elevation of wave runup, may occur more frequently as the foreshore profile adjusts to the daily wave climate. However, use of a mean beach slope (fig. 6) in this analysis provides a more temporally stable estimate of slope and hence a more consistent measure of storm-induced wave runup.

4.2 Relative Importance of Waves and Storm Surge

Hurricane-induced coastal changes are caused by waves and surge and the interaction of these processes with coastal morphology. Waves (setup and swash) were shown to increase water levels at the shoreline by 144 percent for a category 1 storm when compared to considering storm surge alone. Using a regional average of wave height and period for a category 1 hurricane (table 2), the predicted wave-driven component of shoreline water levels, η_{R2} , was 3.76 m, high enough to reach the mean dune toe elevation ($z_t = 2.64$), even without surge. For the category 2 hurricane conditions modeled in this analysis, the wave-driven and storm surge components were similar (3.85 m and 3.56 m, respectively). During a category 4 storm, the magnitude of surge exceeded the wave component; however, the magnitude of runup was 4.14 m, exceeding the dune crest height in nearly half of the area along the northeast Atlantic coast (table 1). This indicates that the waves alone are large enough to make dunes in this area vulnerable to extreme erosion.

4.3 Nor'easters versus Hurricanes

Both hurricanes and nor'easters occur in the north Atlantic and are characterized by strong winds and large waves, and typically are accompanied by heavy precipitation that can cause substantial coastal erosion. Hurricanes are cyclones that form in the tropical waters of the Atlantic and move northwest of their formation location. Hurricanes are strong, well-organized low pressure systems and typically influence a fairly small area, about 150 km (Zhang and others, 2001). Nor'easters are extratropical cyclones that often form along the U.S. mid-Atlantic coast and move northeastward as they strengthen (Butman and others, 2008). Nor'easters are diffuse and weaker low pressure systems in which wind

speeds typically are less than those of a category 1 hurricane (about 33 meters per second). Nor'easters occur more frequently than hurricanes, are much larger in size, and can continue for several days and affect almost the entire U.S. East Coast (Zhang and others, 2001). However, an assessment of the coastal change impacts of nor'easters on these beaches is beyond the scope of this report.

4.4 Coastal Morphology

The Gulf of Mexico, southeast Atlantic, and mid-Atlantic coasts are dominated by sandy beaches. The northeast Atlantic coast, however, has a wide variety of coastal morphologies in addition to sandy beaches including gravel beaches, mixed sediment beaches, rocky coast, and bluff-backed beaches. Gravel beaches are characterized by the predominant grain size having a diameter larger than 2 millimeters. Mixed sediment beaches are defined as sandy beaches with boulders or large rock formations immediately seaward of the beach or on the beach itself. Rock on the beach can minimize the impact of breaking waves on erosion of the sandy beach, but the rock does not markedly affect total water levels on the beach. Because gravel beaches and mixed sediment beaches are susceptible to erosion during storms, they are included in the runup calculations. Gravel beaches are less susceptible to transport and erosion during storms due to their larger mean grain size and therefore have a higher critical threshold for transport (Soulsby and Whitehouse, 1997). On rocky coasts, rock formations take the place of sediment grains, and there is no beach and dune system; therefore, the runup equation does not apply, and these areas are not included in the calculations for coastal erosion. Rocky coasts are prevalent in Maine and along the coast from approximately 100 km north to approximately 15 km south of Boston, Massachusetts.

A roughly 30-km section of the coast along Cape Cod, Massachusetts, is backed by 10 to 50 m tall bluffs. The bluffs are composed of consolidated sands and may be susceptible to erosion at the base. The dune crest in this area was selected as the top of the bluff, and the dune toe was selected as the base of the bluff above the beach berm (if present). Erosion of the bluff is expected during the collision, overwash, and inundation regimes. While the typical effects of overwash or inundation will not occur in these areas because the top of the bluffs should not be affected by waves and surge, it is important to characterize the bluffed beaches as sandy shorelines that are likely to be eroded during storms.

4.5 Assessment Updates

The vulnerability of sandy beaches can be expected to change in the future because of variations in storminess, sea-level rise, and human engineering efforts that alter beach configurations. As new observations and storm predictions become available, assessments may be revised to provide updated probabilities as well as a synthesis of how coastal vulnerability to storms changes in the future (<http://coastal.er.usgs.gov/hurricanes/erosionhazards/>). Specifically, coastal topography is being updated to account for actual storm-driven, or even engineered, changes to the coast associated with hurricane recovery, coastal restoration, and mitigation. This updating process is underway nearly continuously as USGS, USACE, State agencies, and other entities utilize increasingly effective lidar capabilities in acquiring coastal coverage for a variety of needs. Examples of the updates associated with major hurricane landfall can be found at <http://coastal.er.usgs.gov/hurricanes/>.

5. Conclusion

This assessment quantifies the probabilities of dune erosion, dune overwash, and beach/dune inundation during the landfall of category 1–4 hurricanes. The probabilities were calculated by comparing beach/dune elevations to modeled estimates of the hurricane-induced total water level at the shoreline, including contributions from both waves and storm surge. The sandy beaches, coastal infrastructure, and habitat of the northeast Atlantic coast are vulnerable to extreme coastal changes during landfall of even category 1 hurricanes. The severity of these changes increases as the intensity of the storm-driven surge and waves increases and as the height of protective dunes decreases. Citizens and coastal managers who need to understand, plan for, and adapt to different levels of vulnerability will benefit from guidance on the likelihood of encountering mild, moderate, or severe erosion and deposition (overwash) associated with different storm intensities.

By including wave-driven setup and swash in addition to storm surge, we have identified the relative importance of waves in terms of their impact on erosion vulnerability. For category 1 hurricanes in this region, modeled wave runoff is of greater magnitude than storm surge. As storm intensity increases, the relative importance of storm surge grows at a fast rate as nearshore wave height is limited because of dissipation by white-capping and breaking. Analyses that ignore the wave component of this problem will underestimate erosion vulnerability, particularly for lower category hurricanes, tropical storms, nor'easters, or cold fronts.

Though coastal elevations in the northeast Atlantic are somewhat higher than in other areas along the Atlantic and Gulf coasts, the combination of steeper beach slopes and large waves and surges makes the northeast region vulnerable to substantial coastal erosion during storms. In the direct landfall of a category 1 hurricane, 96 percent of dune-backed beaches along the northeast Atlantic coast are very likely ($p > 90$ percent) to experience dune erosion during the collision regime. Overwash during landfall of a category 1 hurricane is very likely along 54 percent of the sandy coastline. During category 4 hurricane conditions, 82 percent of the northeast Atlantic sandy beaches are very likely to experience overwash and associated erosion, and 69 percent of the beaches and dunes are very likely to be vulnerable to erosion caused by inundation.

6. Acknowledgments

The USGS National Assessment of Coastal Change Hazards Project Extreme Storms and Hurricanes group thanks the many scientists and research assistants who have contributed to the research and data collection that made this assessment possible. Online mapping support was provided by Kathryn Smith. We thank the CHARTS program as well as USGS field support and survey teams for the comprehensive lidar dataset that formed the basis of this analysis. John Cannon (National Weather Service) and Tim Nelson (USGS) provided thorough and thoughtful reviews. This research has been supported by the USGS Coastal and Marine Geology Program.

7. References Cited

- Butman B., Sherwood C.R., and Dalyander P.S., 2008, Northeast storms ranked by wind stress and wave-generated bottom stress observed in Massachusetts Bay, 1990–2006: *Continental Shelf Research*, v. 28, p. 1231–1245.
- Cubasch, U., Wuebbles, D., Chen, D., Facchini, M.C., Frame, D., Mahowald, N., and Winther, J.-G., 2013, Introduction, *in* Stocker, T.F., Qin, D., Plattner, G.-K., Tignor, M., Allen, S.K., Boschung, J., Nauels, A., Xia, Y., Bex, V., Midgley, P.M., eds., *Climate change 2013, The physical science basis, Contribution of Working Group I to the Fifth Assessment Report of the Intergovernmental Panel on Climate Change*: Cambridge, Cambridge University Press, 1,535 p.
- Doran, K.S., Stockdon, H.F., Sopkin, K.L., Thompson, D.M., and Plant, N.G., 2013, National assessment of hurricane-induced coastal erosion hazards—Mid-Atlantic Coast: U.S. Geological Survey Open-File Report 2013–1131, 28 p., accessed November 14, 2014, at <http://pubs.usgs.gov/of/2013/1131/>.
- Holthuijsen, L.H., Booij, N., and Ris, R.C., 1993, A spectral wave model for the coastal zone, *in* Wiegel, R.L., Magoon, O.T., and Hemsley, J.M., eds., *Ocean wave measurement and analysis: Proceedings of the Second International Symposium, honoring professor Robert L. Wiegel*, New Orleans, Louisiana, July 25–28, 1993, p. 630–641.
- Houston, S.H., Shaffer, W.A., Powell, M.D., and Chen, J., 1999, Comparisons of HRD and SLOSH surface wind fields in hurricanes—Implications for storm surge modeling: *Weather and Forecasting*, v. 14, p. 671–686.
- Irish, J.L., Resio, D.T., and Ratcliff, J.J., 2008, The influence of storm size on hurricane surge: *Journal of Physical Oceanography*, v. 38, no. 9, p. 2003–2013.
- Irish, J.L., Resio, D.T., and Cialone, M.A., 2009, A surge response function approach to coastal hazard assessment, Part 2—Quantification of spatial attributes of response functions: *Natural Hazards*, v. 51, no. 1, p. 183–205.
- Jarvinen, B.R., and Lawrence, M.B., 1985, An evaluation of the SLOSH storm surge model: *Bulletin of the American Meteorological Society*, v. 66, no. 11, p. 1408–1411.
- National Oceanic and Atmospheric Administration (NOAA), 2007, Hurricane preparedness: SLOSH model, National Hurricane Center. <http://www.nhc.noaa.gov/surge/slosh.php>.
- Plant, N.G., Holland, K.T., and Puleo, J.A., 2002, Analysis of the scale of errors in nearshore bathymetric data: *Marine Geology*, v. 191, no. 1–2, p. 71–86.
- Plant, N.G., and Stockdon, H.F., 2012, Probabilistic prediction of barrier-island response to hurricanes: *Journal of Geophysical Research Earth Surface*, v. 117, F03015, doi:10.1029/2011JF002326.
- Plant, N.G., Stockdon, H.F., Sallenger, A.H., Jr., Turco, M.J., East, J.W., Taylor, A.A., and Shaffer, W.A., 2010, Forecasting hurricane impact on coastal topography: *Eos Transactions American Geophysical Union*, v. 91, no. 7, p. 65–66.

- Ruggiero, P., and List, J.H., 2009, Improving accuracy and statistical reliability of shoreline position and change rate estimates: *Journal of Coastal Research*, v. 25, no. 5, p. 1069–1081.
- Sallenger, A.H., 2000, Storm impact scale for barrier islands: *Journal of Coastal Research*, v. 16, no. 3, p. 890–895.
- Sallenger, A.H., Krabill, W., Swift, R., Brock, J., List, J., Hansen, M., Holman, R.A., Manizade, S., Sontag, J., Meredith, A., Morgan, K., and Stockdon, H., 2003, Evaluation of airborne scanning lidar for coastal change applications: *Journal of Coastal Research*, v. 19, p. 125–133.
- Soulsby, R.L., and Whitehouse, R.J.S., 1997, Threshold of sediment motion in coastal environments, *in* Pacific Coasts and Ports '97, Christchurch, New Zealand, September 7–11, 1997: Proceedings of the 13th Australasian Coastal and Ocean Engineering Conference and the 6th Australasian Port and Harbour Conference, v. 1, p. 145–154.
- Stockdon, H.F., Holman, R.A., Howd, P.A., and Sallenger, A.H., 2006, Empirical parameterization of setup, swash, and runup: *Coastal Engineering*, v. 53, no. 7, p. 573–588.
- Stockdon, H.F., Sallenger, A.H., Holman, R.A., and Howd, P.A., 2007a, A simple model for the spatially-variable coastal response to hurricanes: *Marine Geology*, v. 238, p. 1–20.
- Stockdon, H.F., Thompson, D.M., and Sallenger, A.H., 2007b, Hindcasting potential hurricane impacts on rapidly changing barrier islands, *in* Proceedings, Coastal Sediments '07: Sixth International Symposium on Coastal Engineering and Science of Coastal Sediment Processes, New Orleans, Louisiana, May 13–17, 2007, American Society of Civil Engineers, p. 976–985.
- Stockdon, H.F., Doran, K.S., and Sallenger, A.H., 2009, Extraction of lidar-based dune-crest elevations for use in examining the vulnerability of beaches to inundation during hurricanes: *Journal of Coastal Research*, v. 25, no. 6, p. 59–65.
- Stockdon, H.F., Doran, K.J., Thompson, D.M., Sopkin, K.L., Plant, N.G., and Sallenger, A.H., 2012, National assessment of hurricane-induced coastal erosion hazards—Gulf of Mexico: U.S. Geological Survey Open-File Report 2012–1084, 51 p., accessed November 14, 2014, at <http://pubs.usgs.gov/of/2012/1084/>.
- Stockdon, H.F., Doran, K.S., Sopkin, K.L., Thompson, D.M., and Plant, N.G., 2013, National assessment of hurricane-induced coastal erosion hazards—Southeast Atlantic coast: U.S. Geological Survey Open-File Report 2013–1130, 34 p., accessed November 14, 2014, at <http://pubs.usgs.gov/of/2013/1130/>.
- U.S. Geological Survey, 2014, Coastal change hazards—Hurricanes and extreme storms, St. Petersburg Coastal and Marine Science Center Web site, accessed November 13, 2014, at <http://coastal.er.usgs.gov/hurricanes/>.
- U.S. Geological Survey, Coastal Change Hazards Portal, n.d., accessed November 14, 2014, at <http://marine.usgs.gov/coastalchangehazardsportal/>.
- Zhang, K., Douglas, B.C., Leatherman, S.P., 2001, Beach erosion potential for severe nor'easters: *Journal of Coastal Research* v. 17, p. 309–321.

Tables

Table 1. Mean elevation of dune crest (z_c), dune toe (z_t), and mean beach slope (β_m) for the sandy beaches along the northeast Atlantic coast. [Standard deviation is given in parentheses. m, meter]

State/region	z_c [m]	z_t [m]	β_m	Survey date [month/year]
U.S. northeast Atlantic coast	4.83 (1.81)	2.64 (0.83)	0.088 (0.044)	
Rhode Island	4.09 (0.85)	2.15 (0.40)	0.096 (0.041)	5/2010
Massachusetts	5.19 (2.17)	2.86 (0.95)	0.081 (0.041)	5/2010
New Hampshire	4.49 (0.95)	2.51 (0.35)	0.131 (0.073)	5/2010
Maine	4.45 (0.96)	2.43 (0.45)	0.093 (0.038)	5/2010

Table 2. Mean input wind speed, significant wave height (H_s), wave period (T_p), modeled setup (η_{setup}), runup (η_{R2}), and storm surge (η_{surge}) for category 1–4 hurricanes. [Standard deviation is given in parentheses. m/s, meters per second; m, meter; s, second]

Hurricane intensity category	Wind speed [m/s]	H_s [m]	T_p [s]	η_{setup} [m]	η_{R2} [m]	η_{surge} [m]
1	42.5	8.19 (0.80)	12.34 (0.39)	1.37 (0.70)	3.76 (1.42)	2.62 (0.30)
2	49.2	8.42 (0.83)	12.45 (0.38)	1.40 (0.71)	3.85 (1.44)	3.56 (0.51)
3	58.1	8.81 (0.95)	12.62 (0.41)	1.45 (0.73)	3.98 (1.47)	4.51 (0.69)
4	69.3	9.25 (1.05)	12.81 (0.42)	1.51 (0.75)	4.14 (1.52)	5.44 (0.86)

Table 3. Percentage of coast very likely ($p>0.9$) to experience erosion associated with collision, overwash, and inundation during category 1–4 hurricanes.

	Hurricane intensity category			
	1	2	3	4
Collision				
U.S. northeast Atlantic coast	96	97	98	99
Rhode Island	100	100	100	100
Massachusetts	93	95	97	99
New Hampshire	100	100	100	100
Maine	100	100	100	100
Overwash				
U.S. northeast Atlantic coast	54	69	76	82
Rhode Island	89	97	98	100
Massachusetts	37	53	61	71
New Hampshire	67	83	100	100
Maine	74	93	97	100
Inundation				
U.S. northeast Atlantic coast	13	40	57	69
Rhode Island	24	75	94	98
Massachusetts	8	25	38	53
New Hampshire	17	56	72	78
Maine	20	53	82	92

